Generalized Universal Domain Adaptation with Generative Flow Networks

Didi Zhu *1, Yinchuan Li *2, Yunfeng Shao², Jianye Hao², Fei Wu¹, Kun Kuang¹, Jun Xiao¹, and Chao Wu †1

1,2,3 Zhejiang University, Huawei Noah's Ark Lab, Tianjin University

Abstract

We introduce a new problem in unsupervised domain adaptation, termed as Generalized Universal Domain Adaptation (GUDA), which aims to achieve precise prediction of all target labels including unknown categories. GUDA bridges the gap between label distribution shift-based and label space mismatch-based variants, essentially categorizing them as a unified problem, guiding to a comprehensive framework for thoroughly solving all the variants. The key challenge of GUDA is developing and identifying novel target categories while estimating the target label distribution. To address this problem, we take advantage of the powerful exploration capability of generative flow networks and propose an active domain adaptation algorithm named GFlowDA, which selects diverse samples with probabilities proportional to a reward function. To enhance the exploration capability and effectively perceive the target label distribution, we tailor the states and rewards, and introduce an efficient solution for parent exploration and state transition. We also propose a training paradigm for GUDA called Generalized Universal Adversarial Network (GUAN), which involves collaborative optimization between GUAN and GFlowNet. Theoretical analysis highlights the importance of exploration, and extensive experiments on benchmark datasets demonstrate the superiority of GFlowDA.

1. Introduction

Deep neural networks have been widely employed in various visual tasks and made revolutionary advances [7, 20, 44, 13]. However, deep learning algorithms highly rely on massive labeled data, and models trained with limited labeled data do not generalize well on domains with different

distributions. Unsupervised domain adaptation (UDA) [2] has emerged as a promising solution to address this limitation by adapting models trained on a source domain to perform well on an unlabeled target domain. Recent literature [11, 27, 48, 51, 8, 37, 18, 15, 14] addresses the UDA problem under covariate assumption [57], for which methods perform importance weighting or aim at aligning the marginal distributions in some learned feature space. However, these methods increase the general loss on the target domain when facing label heterogeneity.

UDA variants with label heterogeneity can be categorized based on the variation of label distribution, label space, and label prediction space. The label distribution can be split into conditions ① $P_s(Y) \neq P_t(Y)$ and ② $P_s(X|Y) \neq P_t(X|Y)$. $P_{\{s,t\}}(Y)$ and $P_{\{s,t\}}(X|Y)$ indicate the margin label distribution and the class-conditional distribution, respectively. The label shift (LS) problem [57] corresponds to ①, while the generalized label shift (GLS) problem [57] corresponds to $\textcircled{1} \land \textcircled{2}$. The *label space* can $\overline{\mathcal{Y}}_t \neq \emptyset$ & unknown with $\overline{\mathcal{Y}}_{\{s,t\}}$ denoting the private label space. The *label prediction space*, denoted as $|\widehat{\mathcal{Y}}|$, includes two conditions: § $|\widehat{\mathcal{Y}}| = k+1$, where all target private labels are considered as "unknown"; and $(\hat{\mathcal{Y}}) = k + n$, where k and n denote the size of the common label set and the target private label set, respectively. Partial domain adaptation (PDA) [56] assumes private classes only exist in the source domain (3), while open set domain adaptation (OSDA) [41] assumes they only exist in the target domain ($\P \wedge \P$). Universal domain adaptation (UniDA) [54] is a more general case with no knowledge about the label space relationship, summarized as $3 \land 4 \land 5$.

Label distribution based variants mainly focus on estimating label ratio to reweight source samples, whereas label space based variants are devoted to designing heuristic rules to determine whether the samples belong to the private label set. However, methods for these two types of variants are

^{*} Equal contributions.

[†] Corresponding author.

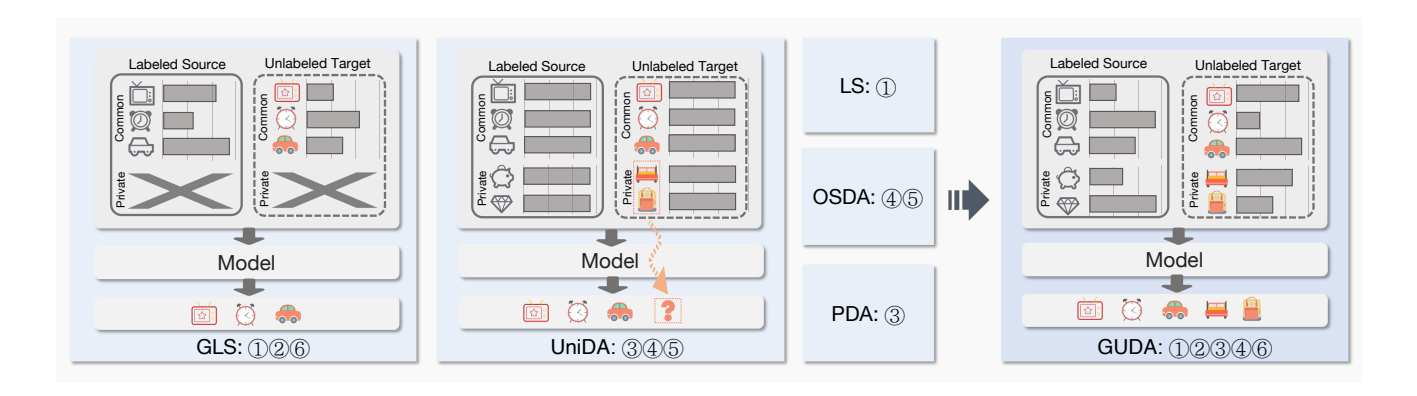


Figure 1: Illustration of GUDA and some subproblems of GUDA. GUDA contains most domain adaptation tasks from the perspective of label distribution, label space and label prediction space.

often incapable of resolving one another, despite that their fundamental requirements are both to fully explore the target labels. In practice, it is difficult to identify which variant is being encountered, and real-world scenarios may involve a combination of these variants, making it challenging to apply any single method. Furthermore, the label space based variants can only identify unseen categories as "unknown", limiting their ability to achieve fine-grained recognition and failing to meet practical needs. These dilemmas highlight the necessity for a unified framework to address both label distribution and label space variants, while also enabling fine-grained prediction of unknown target categories.

In this paper, we propose a new problem Generalized Universal Domain Adaptation (GUDA) to take a unified view of these above problems, as illustrated in Fig. 1, which can be represented as $\textcircled{1} \land \textcircled{2} \land \textcircled{3} \land \textcircled{4} \land \textcircled{6}$. The key challenge of GUDA is developing and identifying novel categories that exist in the target domain while estimating the overall label distribution for subsequent feature alignment. To address GUDA, we take the benefit of the powerful exploration capability of Generative Flow Networks (GFlowNets) [3] and propose an active domain adaptation framework named **GFlowDA**, which could explore the overall target label distribution by annotating a subset of target data. Unlike the previous active domain adaptation (ADA) works [10, 34, 52, 29, 16, 53, 6], which either focus on designing metrics [29, 9, 53] that may have some bias or minimizing the feature distance while easily falling into the trap of sub-optimal solutions [16, 6, 34, 52], our insight is to learn a generative policy that generates a distribution with probabilities proportional to the distance of the original target distribution. We consider the selected target subset as a compositional object and formulate the ADA problem as a distribution generative process by sequentially selecting a target sample through GFlowNets. To facilitate GFlowNets to better perceive the target label distribution, we customize

the states and rewards, and introduce an efficient parent exploration and state transition approach. Finally, we propose a novel weighted adaptive model named Generalized Universal Adversarial Network (GUAN), which enables efficient domain alignment through a reciprocal relationship between GFlowNets and GUAN.

Main Contribution: (1) We introduce GUDA, which covers most UDA variants with label heterogeneity and aims to recognize all target classes including unknown classes. (2) To address this challenge, we propose GFlowDA to select and annotate target samples to estimate the overall target label distribution. (3) We define the design paradigm for states and rewards, and introduce an efficient solution for parent exploration and state transition in the GFlowDA training process. We also propose a new training paradigm for GUDA called GUAN, which involves collaborative optimization between GUAN and GFlowNet. (4) We extend the existing theoretical analysis to GUDA, thus offering crucial theoretical insights for GFlowDA. (5) Extensive experiments show that our GFlowDA achieves a significant improvement over the traditional SOTA algorithms.

2. Related Works

2.1. Unsupervised Domain Adaptation

For LS and GLS problems in the literature of UDA, most works [47,43,21,19,36,58] seek to estimate the label ratio $P_t(Y)/P_s(Y)$ to weight the source feature, which requires that the source label distribution $P_s(Y)$ cannot be zero. This underlying constraint limits the generalization of the methods for LS and GLS to OSDA [41,31] and UniDA [54] scenarios due to the existence of target private labels. Numerous methods for OSDA and UniDA either utilize prediction uncertainty [40,14,54,9,26,39], or incorporate self-supervised learning techniques [1,38,23]. However, these methods often fail to explore fine-grained discrimi-

native knowledge in the unknown set and do not take label distribution shift into account within the common label space. Additionally, most PDA methods [5, 56, 25] aim to weight source samples with heuristic criteria, which suffe from the same limitations as OSDA and UniDA. While recent methods such as OSLS [12] and AUDA [29] have attempted to address some of the above limitations, they may not be entirely suitable for GUDA. Further research is needed to develop more effective methods that can overcome the challenges posed by GUDA.

2.2. Generative Flow Networks

GFlowNets [4] is a generative model which aims to solve the problem of generating diverse candidates. It has been effective in various fields such as molecule generation [3, 30, 17], discrete probabilistic modeling [55] and graph neural networks explanation [24]. Compared to reinforcement learning (RL) methods [46], which focus on maximizing the expected return by generating a sequence of actions with the highest reward, GFlowNets offer the ability to explore diverse reward distributions by sampling trajectories with probabilities proportional to the expected rewards. This feature allows for more effective estimation of the target distribution, making GFlowNets particularly well-suited for GUDA. Subsequent experiments will further analyze the differences between RL and GFlowNets.

2.3. Active Domain Adaptation

The pioneering study [35] demonstrates how active learning (AL) and DA can collaborate to enhance AL in DA. Recent efforts [45, 10, 52] design some criterion by introducing advanced techniques like adversarial training, multiple discriminators and free energy model. Besides, some parallel works [34, 29] suggest using clustering to choose active samples. In addition, distance-based works [6, 16, 53, 34, 29] choose samples based on their distance to the source or the target domain. Overall, existing works mainly rely on manually-designed criteria or distance, leading to overfitting to specific transfer scenarios and easily falling into the trap of sub-optimal solutions. Unlike the existing ADA methods, we consider the query batch as a compositional object and formulate the ADA as a generative process. The generative policy network can automatically explore how to find the most informative samples in an essential way.

3. Problem Formulation

3.1. Notation

Denoting \mathcal{X} , \mathcal{Y} , \mathcal{Z} as the input space, label space and latent space, respectively. Let X, Y and Z be the random variables of \mathcal{X} , \mathcal{Y} , \mathcal{Z} , and x, y and z be their respective elements. Let P_s and P_t be the source distribution and target distribution. We are given a labeled source domain $\mathcal{D}_s = \mathcal{D}_s$

 $\{x_i,y_i\}_{i=1}^m$ and an unlabeled target domain $\mathcal{D}_t=\{x_i\}_{i=1}^n$ are respectively sampled from P_s and P_t , where m and n denote the numbers of source samples and target samples. Denote \mathcal{Y}_s and \mathcal{Y}_t as the label sets of the source and target domains, respectively. Suppose the feature transformation function is $g:\mathcal{X}\to\mathcal{Z}\subseteq\mathbb{R}^{d_z}$ where d_z is the length of each feature vector, and the discrimination function of the label classifier is $h:\mathcal{Z}\to\mathcal{Y}$.

3.2. Problem Formulation

Given $\mathcal{Y}_c = \{1,2,\ldots,k\}$ as the common label space between the source and target domain. We denote $\overline{\mathcal{Y}}_t = \{k+1,\ldots,k+n\}$ as the target private label space and $\overline{\mathcal{Y}}_s$ the source private label space, i.e., $\mathcal{Y}_s = \mathcal{Y}_c \cup \overline{\mathcal{Y}}_s$, $\mathcal{Y}_t = \mathcal{Y}_c \cup \overline{\mathcal{Y}}_t$. Then we have GUDA in Definition 1.

Definition 1 (GUDA). *GUDA is characterized by conditions* $\textcircled{1} \wedge \textcircled{2} \wedge \textcircled{3} \wedge \textcircled{4} \wedge \textcircled{6}$, *i.e.*,

$$P_s(X|Y) \neq P_t(X|Y) > 0, \ P_s(Y) \neq P_t(Y) > 0, \ \exists Y \in \mathcal{Y}_c,$$

and $\overline{\mathcal{Y}}_s \neq \emptyset, \ \overline{\mathcal{Y}}_t \neq \emptyset, \ |\widehat{\mathcal{Y}}| = k + n,$

$$\tag{1}$$

where $\overline{\mathcal{Y}}_s$ and $\overline{\mathcal{Y}}_t$ are both unknown.

GUDA focuses on predicting all target labels, including the private label set, while also accounting for unknown label spaces and generalized label shift. Therefore, the target risk of GUDA can be divided into two parts: the target common risk for classifying common classes and the refined target private risk for classifying the target private classes:

$$\epsilon_{t}(h \circ g) = \mathbb{E}_{(X,Y) \sim \mathcal{D}_{t}} \ell(h \circ g(X), Y) \tag{2}$$

$$= \underbrace{\sum_{i=1}^{k} P_{t}(Y = i) \epsilon_{s,i}(h \circ g)}_{\text{target common risk}} + \underbrace{\sum_{j=k+1}^{k+n} P_{t}(Y = j) \epsilon_{s,j}(h \circ g)}_{\text{refined target private risk}}.$$

To minimize the target risk, an active learning strategy can be employed to annotate a small portion of the target dataset to recover the target distribution. We denote $\mathcal{D}_l = (x_i, y_i)_{i=1}^b$ as the selected labeled target dataset and the probability distribution of \mathcal{D}_l as P_l .

4. Method

4.1. Towards GUDA from a Theoretical View

To start with, we provide a theoretical analysis of the proposed GUDA. First, we introduce the definitions of two performance metrics for the predictor $h \circ g$:

Definition 2 (Balanced Error Rate [47]). Given a distribution P_s , the balanced error rate (BER) of a predictor $h \circ g$ on P_s is given by:

$$\varepsilon_s(\widehat{Y}||Y) := \max_{j \in \mathcal{Y}} P_s(\widehat{Y} \neq Y \mid Y = j),$$

where
$$\widehat{Y} = h \circ g(X)$$
.

Definition 3 (Conditional Error Gap [47]). Given two distributions P_s and P_t , the conditional error gap (CEG) of a classifier $h \circ g$ on P_s and P_t is given by

$$\Delta_{s,t}(\widehat{Y}||Y) := \max_{j \neq i \in \mathcal{Y}} |P_s(\widehat{Y} = i|Y = j) - P_t(\widehat{Y} = i|Y = j)|.$$

BER measures max prediction error on P_s , reflecting the classification performance of a single domain. CEG characterizes the max discrepancy between the classifier's predictions on P_s and P_t , reflecting the degree of conditional feature alignment across domains.

Then we present the target risk upper bound for GUDA in Theorem 2 based on these two definitions, proved in the appendix.

Theorem 1 (Target Risk Upper Bound for GUDA). Let Y_c , Y_l and \overline{Y}_t be random variables taking values from \mathcal{Y}_c , \mathcal{Y}_l and $\overline{\mathcal{Y}}_t$ respectively, with \mathcal{Y}_l being the selected target label space. For any classifier $\hat{Y} = (h \circ g)(X)$, we have

$$\epsilon_t(h \circ g) \leq \epsilon_s(h \circ g) + \epsilon_l(h \circ g) + \delta_{s,t} + \delta_{l,t} + \varepsilon_t(\widehat{Y}||\overline{Y}_t),$$

where

$$\delta_{s,t} = \|P_s(Y_c) - P_t(Y_c)\|_1 \cdot \varepsilon_s(\widehat{Y}||Y_c) + 2(k-1)\Delta_{s,t}(\widehat{Y}||Y_c)$$

$$\delta_{l,t} = \|P_l(Y_l) - P_t(Y_l)\|_1 \cdot \varepsilon_l(\widehat{Y}||Y_l) + 2(v-1)\Delta_{l,t}(\widehat{Y}||Y_l)$$

with $k = |\mathcal{Y}_c|$ and $v = |\mathcal{Y}_l|$, $||P_s(Y_c) - P_t(Y_c)||_1 = \sum_{i \in \mathcal{Y}_c} |P_s(Y=i) - P_t(Y=i)|$ being the L_1 distance between $P_s(Y)$ and $P_t(Y)$ on the common label space \mathcal{Y}_c .

Remark 1. The upper bound $\epsilon_t(h \circ g)$ contains five terms. The first two terms represent the source risk on \mathcal{Y}_c and the selected target risk on \mathcal{Y}_l . The third and fourth terms contain $\|P_s(Y_c) - P_t(Y_c)\|_1$ and $\|P_l(Y_l) - P_t(Y_l)\|_1$ respectively, which both measure the distances of the marginal label distributions across domains. The former is a constant that only depends on \mathcal{D}_s and \mathcal{D}_t while the latter changes dynamically since the construction of \mathcal{D}_l varies with the active learning strategy. $\varepsilon_a(\cdot)$ with $a \in \{s, l, t\}$ in the last three terms measure classification performance on the corresponding domains. $\Delta_{a,t}(\cdot)$ with $a \in \{s, l\}$ in the third and fourth terms measures the performance discrepancy between $P_a(Y)$ and $P_t(Y)$.

The difficulty in minimizing the upper bound stems from the unknown nature of the target label distribution $P_t(Y_t)$ and the label space \mathcal{Y}_t . One potential solution is to minimize the label distribution distance $|P_t(Y_t) - P_t(Y_t)|_1$ while making $|\mathcal{Y}_t|$ close to $|\mathcal{Y}_t|$. To achieve this goal, it is crucial to develop an effective active learning strategy to select informative and representative samples for constructing \mathcal{D}_t that preserves the entire target label distribution and label space.

By doing so, \mathcal{Y}_l can be considered a proxy of \mathcal{Y}_t and P_l a proxy of P_t . We propose GFlowDA based on a GFlowNet generator to generate \mathcal{D}_l by sequentially adding one sample at each step until the budget is used up. We give the formal definition of GFlowDA in Definition 4.

Definition 4 (GFlowDA). Given a source distribution P_s and a target distribution P_t , GFlowDA aims to find the best forward generative policy $\pi(\theta)$ based on flow network to generate a distribution P_l automatically, which can serve as a proxy of P_t . The probability of sampling the distribution P_l satisfies

$$\pi(P_l;\theta) \propto r(P_s, P_t, P_l),$$
 (3)

where θ is the parameter of flow network, $r(\cdot)$ is the reward function based on P_s , P_t and P_l .

4.2. DAG Construction of GFlowDA

Following Bengio et al. [4], consider a direct acyclic graph (DAG) $\mathcal{G}=(\mathcal{S},\mathcal{A})$, where \mathcal{S} and \mathcal{A} are state/node and action/edge sets, respectively. Elements of them at step t are denoted as s_t and a_t ¹ The complete trajectory is a sequence of states $\tau=(s_0,\ldots,s_f)$. To construct \mathcal{G} , we first define the state, action and reward function.

Definition 5 (State). A state $s_t \in S \subseteq \mathbb{R}^{n \times 4}$ in GFlowDA at step t describes the entire target information based on \mathcal{D}_t and the currently labeled data \mathcal{D}_l , where $s_t = \{s_t^i\}_{i=1}^n$ and s_t^i is the state representation of the i-th target sample.

We use $s_t^i(a), a \in \{0,1,2,3\}$ denotes the a-th column of the state matrix. The first column of the state denotes the maximum similarity between target features and selected target features at step t. Intuitively, selecting samples with low maximum similarity values can ensure the instance-level diversity, i.e.,

$$s_t^i(1) = \max_{x_i \in \mathcal{D}_t} \cos(g(x_i), g(x_i)). \tag{4}$$

The second column of the state denotes the maximum similarity between target features and active target prototypes, which ensures class-level diversity, i.e.,

$$s_t^i(2) = \max_{j \in \mathcal{Y}_l} \cos(g(x_i), \mu_l^j), \tag{5}$$

where μ_l^j is the prototype of class j in \mathcal{D}_l , calculated as follows:

$$\mu_l^j = \frac{\sum_{(x,y)\in\mathcal{D}_l} \mathbb{1}\{y=j\}g(x)}{\sum_{(x,y)\in\mathcal{D}_l} \mathbb{1}\{y=j\}}.$$
 (6)

The third column of the state denotes the uncertainty of the target samples, which is calculated by the entropy of the label probabilities $\hat{y}_i = h \circ g(x^i)$, i.e.,

$$s_t^i(3) = H(\hat{y}_i). \tag{7}$$

 $[\]overline{\ }^{1}$ Unless otherwise specified, the subscript "t" denotes "step" when used in conjunction with "s" and "a", and "target" when used in conjunction with "x" and " \mathcal{D} ".

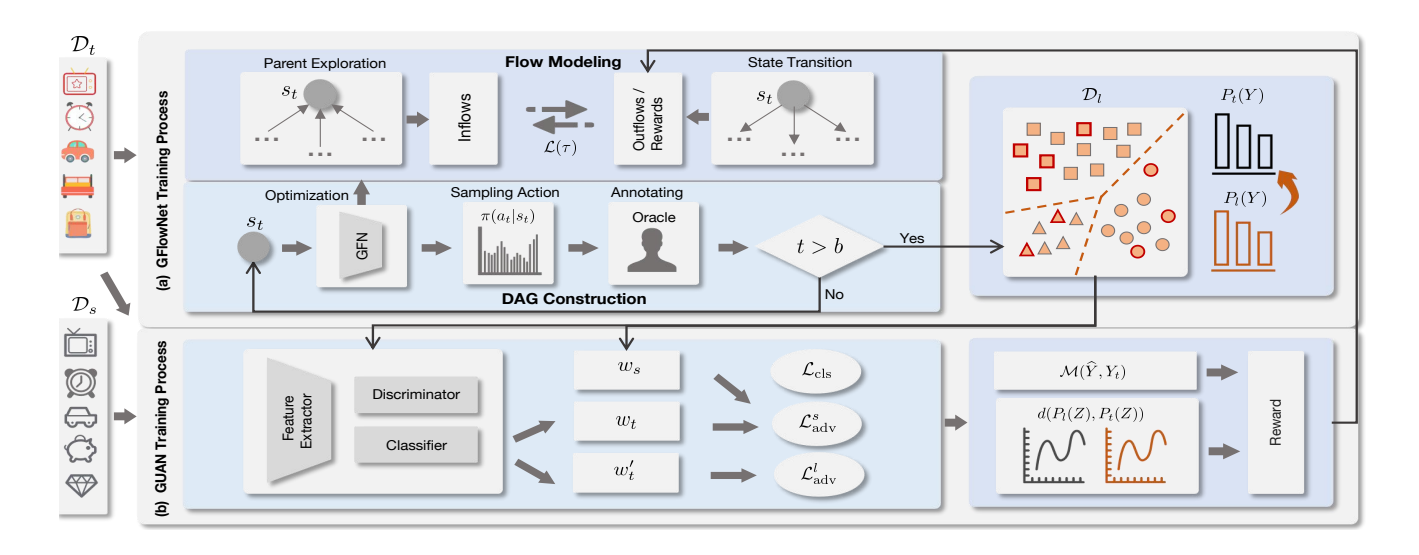


Figure 2: Overall framework of GFlowDA. GFlowNet selects and labels target samples, which are then fed as \mathcal{D}_l to GUAN. GUAN is optimized based on \mathcal{D}_l , \mathcal{D}_s and \mathcal{D}_t . The resulting reward is fed back to GFlowNet, which is then optimized by combining the reward with the inflows and outflows obtained through the parent exploration and state transition process.

The last column of the state is an indicator variable to represent whether a sample has been labeled or not, i.e.,

$$s_t^i(4) = \mathbb{1}\{x^i \in \mathcal{D}_l\}.$$
 (8)

Definition 6 (Action). An action $a_t \in A$ at step t in GFlowDA determines which target instance will be selected from candidate target dataset $\mathcal{D}_t \setminus \mathcal{D}_l$.

Definition 7 (Reward Function). A reward function $r(s_f)$ of the terminal state s_f in GFlowDA refers to a comprehensive metric measuring the quality of \mathcal{D}_l , by taking into account the diversity and informativeness, which is expressed as:

$$r(s_f) = -\operatorname{MMD}(g(X_t), g(X_l) + \mathcal{M}(\widehat{Y}, Y_t),$$
 (9)

where $\widehat{Y} = h \circ g(X)$, MMD(·) represents the Maximum Mean Discrepancy (MMD) [28] between the source and target marginal feature, and $\mathcal{M}(\cdot)$ means the classification accuracy used to evaluate the performance of $h \circ q$.

Remark 2. MMD distance can encourage diverse sample selection that preserves the entire target distribution. To make the selected samples more informative, we incorporate the classification accuracy of the model on the target domain as part of the reward.

By following this design paradigm, we can ensure that the constructed DAG is well-defined and satisfies the acyclic property. This is important because it allows GFlowDA to learn effective policies to achieve optimal distribution generation for GUDA.

4.3. Flow Modeling of GFlowDA

To achieve Eq. 3, a non-negative function $F(\cdot)$ is introduced to measure the probabilities associated with s_t , where $F(s_t, a_t) = F(s_t \to s_{t+1})$ corresponds to an action/edge flow. The trajectory flow is denoted as $F(\tau)$ and the state flow is the sum of all trajectory flows passing through that state, denoted as $F(s) = \sum_{s \in \tau} F(\tau)$. Our objective is to ensure that the DAG $\mathcal G$ operates analogously as a water pipe, where water enters at s_0 and flows out through all s_f , satisfying the condition $F(s_0) = \sum F(s_f) = \sum r(s_f)$. To achieve this, we need to calculate the inflows and outflows of each state, corresponding to the parent exploration and state transition, respectively. As illustrated in Fig. 3, in the parent exploration process, we explore all direct parent states of s_t , i.e., $s \in \mathcal S_p(s_t)$ with $\mathcal S_p(s_t)$ being the parent set. We have the following proposition to guide the exploration procedure:

Proposition 1. For a state s_t in GFlowDA, the number of its parent nodes is equal to the number of labeled samples currently, i.e., $|S_n(s_t)| = ||s_t(4)||_0$.

Based on Proposition 1, one of s_t 's parents is obtained by three steps: (a) selecting the j-th element in the vector $s_t(4)$ and setting its value from 1 to 0 to obtain a new vector $s_{t-1}(4)$, (b) updating the instance-level similarity and (c) updating the class-level similarity based on $s_{t-1}(4)$. Notably, $s_t(3)$ remains fixed as the domain adaptation model updates only at the terminal state. However, directly computing all parent states using Eq.4 and Eq.5 is too time-consuming. Therefore, we propose a more efficient approach to update the similarities. For instance-level similarity, we pre-calculate a cosine similarity matrix $SIM(X_t)$ between

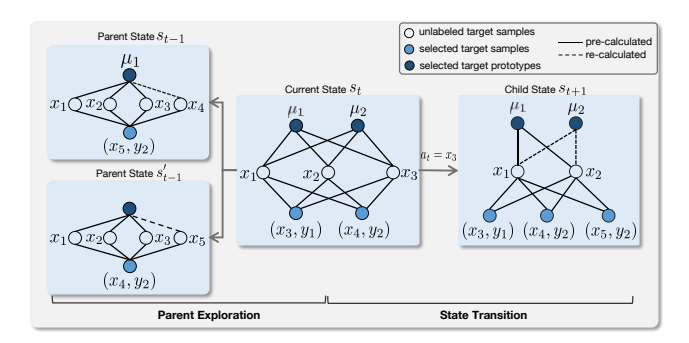


Figure 3: Illustration of efficient parent exploration and state transition. **Left:** At state s_t , x_3 and x_4 are labeled as y_1 and y_2 , resulting in two parent states. **Right:** Due to $a_t = x_3$, x_3 is labeled at s_{t+1} , and the corresponding prototype μ_2 needs to be updated.

all target domain samples at the start of the generative process. The state of the i-th target sample in the first column can be updated as follows.

$$s_{t-1}^{i}(1) = \max(s_{t}^{i}(1), SIM_{i,j}),$$
 (10)

where $\mathrm{SIM}_{i,j}$ denotes the similarity between the i-th target sample and the j-th target sample. For class-level similarity, we just need to update μ^c_t with c being the label of the selected j-th sample. μ^c_{t-1} can be quickly calculated based on μ^c_t , which is given by

$$\mu_{t-1}^{c} = \frac{\mu_{t}^{c} \cdot (\sum_{x \in \mathcal{D}_{t}} \mathbb{1}\{y = c\}) - g(x_{j})}{\sum_{x \in \mathcal{D}_{t}} \mathbb{1}\{y = c\} - 1}.$$
 (11)

Then the state of the i-th target sample in the second column can be updated as follows:

$$s_{t-1}^{i}(2) = \max(s_{t}^{i}(2), \cos(\mu_{t-1}^{c}, x_{i})).$$
 (12)

In the state transition process, if s_t is not a terminal state, we update the dynamic features of s_t to obtain its child state s_{t+1} . This process can be considered an inverse repetition of the parent exploration process. Specifically, once $a_t = j$ is sampled, the j-th element in vector $s_t(4)$ is updated from 0 to 1, resulting in a new vector $s_{t+1}(4)$. Based on $s_{t+1}(4), s_{t+1}(1)$ can be updated by utilizing Eq. 10. To update $s_{t+1}(2)$, we use a similar equation as Eq.12. Since we need to add a new sample instead of removing one as in Eq.11, μ_{t+1}^c is updated as follows:

$$\mu_{t+1}^{c} = \frac{\mu_{t+1}^{c} \cdot (\sum_{x \in \mathcal{D}_{l}} \mathbb{1}\{y = c\}) + g(x_{j})}{\sum_{x \in \mathcal{D}_{l}} \mathbb{1}\{y = k\} + 1}.$$
 (13)

Overall, efficient exploration reduces complexity and accelerates the training of the generative policy network with flow matching loss (discussed in the next subsection).

4.4. Training Procedure

As illustrated in Fig. 2, GFlowDA consists of two primary components: a generative policy network for selecting and annotating the most useful target samples, and a domain adaptation network that utilizes the annotated samples to adapt the target domain.

Genrative Policy Network. Based on the parent set $\mathcal{S}_p(s_t)$ and child set $\mathcal{S}_c(s_t)$ obtained through the above exploration and transition process, we can calculate the corresponding *inflows* and *outflows*. The inflows are calculated by $\sum_{s \in \mathcal{S}_p(s_t)} F(s)$, which represents the sum of action flows from all parent states. The outflows are flows passing through it, which is given by $\sum_{s \in \mathcal{S}_c(s_t)} F(s)$. Starting from an empty set, GFlowDA draws complete trajectories $\tau = (s_0, s_1, \ldots, s_f)$ by iteratively sampling target samples until the budget is used up. After sampling a buffer, we train the policy $\pi(\theta)$ to satisfy Eq. 3, by minimizing the loss over the flow matching condition:

$$\mathcal{L}(\tau) = \sum_{s_t \in \tau \neq s_0} \left\{ \log \left[\epsilon + \sum_{s \in \mathcal{S}_p(s_t)} F' \right] - \log \left[\epsilon + \mathbb{1}_{s_t = s_f} r(s_f) + \mathbb{1}_{s_t \neq s_f} \sum_{s \in \mathcal{S}_c(s_t)} F' \right] \right\}^2,$$
(14)

where $F' = \exp(\log F(s))$, and the reward $r(s_f)$ is computed by Eq. 9. For internal states, we only calculate outflows based on action distributions. For terminal states, we calculate their rewards to evaluate the efficacy of \mathcal{D}_l . To acquire a dependable reward, we introduce a new domain adaptation network as follows.

Generalized Universal Adversarial Network. In the GFlowDA framework, we propose a novel weighted adaptive model for GUDA named Generalized Universal Adversarial Network (GUAN). In addition to the feature extractor g and classifier h, GUAN also includes a domain discriminator $d: \mathcal{Z} \to \mathbb{R}$, which aims to align the source and target features adversarially. The weighted alignment losses of source data and labeled target data are formally described as follows

$$\mathcal{L}_{\text{adv}}^{s} = -\mathbb{E}_{x \sim P_{s}} w_{s} \log \left(d(z) \right) - \mathbb{E}_{x \sim P_{t}} w_{t} \log \left(1 - d(z) \right)$$

$$\mathcal{L}_{\text{adv}}^{l} = -\mathbb{E}_{x \sim P_{t}} \log \left(d(z) \right) - \mathbb{E}_{x \sim P_{t}} w_{t}' \log \left(1 - d(z) \right) ,$$

$$(16)$$

where z = g(x). w_s in Eq. 15 indicates the ratio between the estimated target label distribution and the source label distribution if x is determined to belong to \mathcal{Y}_c , which is defined as follows:

$$w_s = \mathbb{1}(y \in \mathcal{Y}') \cdot (P_l(y)/P_s(y)) + (1 - \mathbb{1}(y \in \mathcal{Y}')) \cdot \lambda$$

where $\mathcal{Y}' = \mathcal{Y}_l \cap \mathcal{Y}_s$ acting as an approximation of the common label space \mathcal{Y}_c , and λ is a constant working as a

Table 1: Average class accuracies (%) and JSD (%) on Office-31 with 5% target data as the labeling budget.

Malad	A	\rightarrow D	Α -	→ W	D -	→ A	D -	→ W	W -	→ A	W -	→ D	l A	vg
Method	Acc	JSD	Acc	JSD	Acc	JSD	Acc	JSD	Acc	JSD	Acc	JSD	Acc	JSD
Random	46.23	16.22	60.79	15.80	55.67	3.14	67.98	14.39	61.80	3.57	67.46	15.64	59.99	11.46
Entropy [50]	53.85	27.93	57.12	23.53	65.88	15.09	70.12	22.96	67.16	4.93	70.91	35.04	64.17	21.58
TQS [10]	63.10	16.02	67.80	15.92	65.72	2.67	82.40	16.84	66.85	3.01	80.65	21.93	71.09	12.73
CLUE [34]	56.89	23.96	66.12	15.36	61.01	3.97	81.37	16.39	60.13	7.23	75.27	22.06	66.80	14.83
EADA [52]	46.63	27.15	65.40	21.10	51.05	7.60	72.40	28.39	54.22	7.11	73.02	22.93	60.45	19.05
SDM-AG [53]	62.76	22.85	68.20	17.38	65.3	5.67	79.40	21.42	64.41	3.49	72.43	25.87	68.75	16.11
AUDA [52]	65.13	21.36	67.36	18.32	67.12	5.01	79.60	20.87	63.78	4.12	77.14	19.36	70.02	14.84
RLADA (Ours)	67.36	20.33	71.23	16.79	70.56	3.67	79.88	16.03	65.98	3.20	76.78	19.66	71.96	13.28
GFlowDA (Ours)	70.50	15.01	73.00	13.54	74.80	1.72	82.60	11.93	67.51	1.51	80.75	14.40	74.86	9.68

Table 2: Average class accuracies (%) and JSD (%) on **Office-Home** with 5% target data as the labeling budget.

Method	Ar-	→ Cl JSD	Ar— Acc	→ Pr JSD	Ar— Acc	→ Rw JSD	Cl— Acc	→ Ar JSD	Cl– Acc	→ Pr JSD	Cl—:	→ Rw JSD	Avg (12	2 tasks) JSD
Random	38.80	7.24	63.92	6.06	63.67	6.91	42.38	12.14	61.69	5.47	65.48	5.40	52.20	7.76
Entropy [50]	37.39	8.79	65.79	7.20	57.75	22.09	38.52	14.70	56.22	10.92	55.37	12.49	48.36	14.72
TQS [10]	43.55	6.15	68.94	8.38	64.47	5.37	39.39	11.37	59.63	6.12	54.00	7.74	52.49	8.04
CLUE [34]	42.14	7.12	70.12	5.88	65.12	4.78	41.57	7.54	63.11	7.23	56.23	7.17	53.98	7.16
EADA [52]	40.36	5.65	69.06	7.44	62.19	6.17	30.67	10.68	65.14	9.47	54.53	7.64	50.28	9.32
SDM-AG [53]	40.01	8.43	69.25	7.99	62.26	8.54	38.21	9.74	53.13	10.98	51.51	9.78	42.84	10.83
LAMDA [16]	42.19	8.59	59.75	7.22	70.51	9.25	44.80	17.49	67.17	6.21	52.47	10.21	53.86	11.37
RLADA (Ours) GFlowDA (Ours)	47.56 51.89	7.12 5.01	72.69 74.77	6.73 4.87	65.81 72.99	7.33 5.46	40.37 44.23	10.67 7.12	66.52 72.29	8.64 6.18	60.46 67.11	6.48 5.03	55.32 59.32	7.68 5.65

remedy for compatibility with the potential inconsistency between \mathcal{Y}' and \mathcal{Y}_c .

 $w_t(x)$ in Eq. 15 and $w_t'(x)$ in Eq. 16 indicate the probability of a target sample x belonging to the source label set \mathcal{Y}_s and the selected labeled target label set \mathcal{Y}_t , respectively. We use the predicted probabilities over all labels in \mathcal{Y}_s and \mathcal{Y}_t respectively to estimate the probabilities, as described below:

$$w_t = \frac{1}{u} \sum_{i \in \mathcal{V}_s} \hat{\boldsymbol{y}}[i], \quad w_t' = \frac{1}{v} \sum_{i \in \mathcal{V}_t} \hat{\boldsymbol{y}}[i]$$
 (17)

where $k=|\mathcal{Y}_c|$ and $v=|\mathcal{Y}_l|$, $\hat{\boldsymbol{y}}=h(z)$ represents the prediction probability vector.

The classification loss for GUAN aims to minimize the cross-entropy loss for both source and labeled target samples:

$$\mathcal{L}_{cls} = -\mathbb{E}_{x \sim P_s} L\left(\hat{y}, y\right) - \mathbb{E}_{x \sim P_t} L\left(\hat{y}, y\right), \tag{18}$$

where $\hat{y} = h \circ g(x)$ and $L(\cdot)$ is the cross entropy loss.

In GFlowDA, the generative policy network is updated through the reward computed by GUAN and then generates new selected target dataset \mathcal{D}_l , which in turn updates GUAN. This reciprocal relationship between the generative policy network and GUAN makes it possible to achieve efficient alignment between domains while improving the classification accuracy of the GUDA task.

5. Experiments

5.1. Experimental Setup

Datasets. We perform experiments on five benchmarks including Office-31 [37], Office-Home [49], PACS [22], VisDA [33] and DomainNet [32]. To evaluate our algorithm on GUDA, we modify the source and target dataset by combining two subsampling protocols [54, 47]. These protocols are tailored for GLS and UniDA respectively. See the appendix for more details.

Comparison Baselines. We compare our method against several state-of-the-art AL methods and ADA methods including (1) Random, (2) Entropy [50], (3) TQS [10], (4) CLUE [34], (5) EADA [52], (6) SDM-AG [53], (7) LAMDA [16]. Furthermore, to illustrate the superiority of GFlowDA, we also implemented a new algorithm by changing the policy network from GflowNet to Proximal Policy Optimization [42] and keeping everything else the same, named (8) Reinforcement Learning Active Domain Adaptation, abbreviated as RLADA.

Evaluation metrics. Besides reporting the average class accuracy, we also compared the Jensen-Shanon divergence (JSD) between the label distribution of the selected samples and the original target samples, denoted by $d_{\rm JS}(P_l^Y,P_t^Y)$. The JSD value can provide an intuitive reflection of the label distribution reduction and exploration ability of AL strategies. A smaller JSD value indicates that the selected samples are better able to estimate the original target distribution.

Table 3: Average class accuracies (%) and JSD (%) on PACS and with 1% target data as the labeling budget.

	1	PACS (%)													
Method	A -	→ C	Α –	→ P	A -	→ S	C -	→ A	C -	\rightarrow P	Avg (1	2 tasks)	S-	+ R	
	Acc	JSD	Acc	JSD	Acc	JSD	Acc	JSD	Acc	JSD	Acc	JSD	Acc	JSD	
Random	52.80	0.29	81.86	9.69	60.24	1.58	58.35	0.02	82.80	11.98	63.27	4.30	55.52	0.46	
Entropy [50]	44.53	3.05	67.01	15.58	60.65	1.42	35.71	5.99	84.44	16.94	58.38	8.20	50.45	8.42	
TQS [10]	63.82	5.82	83.89	5.71	80.43	2.77	44.48	4.39	87.65	3.47	63.12	6.37	82.87	5.10	
EADA [52]	35.18	9.01	28.46	34.67	38.21	5.42	23.97	7.67	40.66	26.67	34.38	11.16	84.73	1.98	
SDM-AG [53]	68.76	3.91	90.63	7.81	84.03	2.39	51.63	2.55	74.90	6.73	63.16	4.18	80.69	2.60	
LAMDA [16]	53.20	1.62	82.67	6.66	55.87	2.96	58.81	1.04	91.08	9.81	65.97	5.85	-	-	
RLADA (Ours)	59.78	3.28	90.12	4.32	67.03	0.80	57.03	2.78	87.21	4.07	66.00	2.94	81.23	3.23	
GFlowDA (Ours)	64.34	1.06	91.38	4.11	67.23	0.55	56.66	0.61	90.54	1.87	68.26	1.93	85.23	1.03	

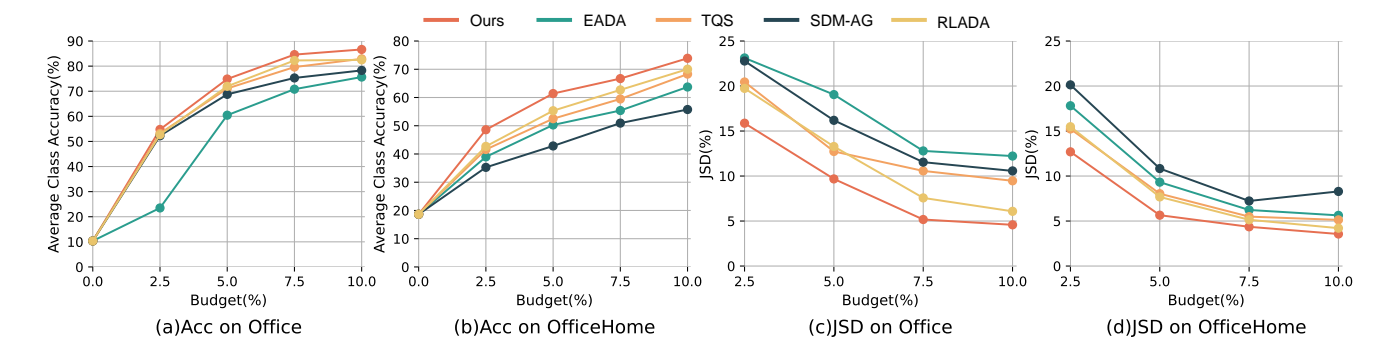


Figure 4: Average class accuracies (%) and JSD (%) on Office-31 and Office-Home with different budget.

5.2. Main Results of GFlowDA

Performance of GFlowDA on GUDA. The experimental results of different methods with 5% labeling budget on Office-31, Office-Home, PACS and VisDA are shown in Table 1, Table 2 and Table 3 respectively, demonstrating that GFlowDA surpasses all the active learning and active domain adaptation baselines by a large margin in both accuracy and JSD. More results on DomainNet are available in the appendix. It is worth noting that the random strategy outperforms most heuristic rule-based methods in terms of JSD, which is statistically intuitive that random sample selection is an independent and identically distributed (i.i.d.) procedure w.r.t. the original target distribution. However, random selection can be unstable and does not guarantee informative samples, which may explain why it achieves comparable JSD but 14.87% lower accuracy than GFlowDA on Office-31. Furthermore, two learning-based active strategies, GFlowDA and RLADA, achieve optimal and suboptimal accuracy on Office-31, Office-Home and PACS, indicating that such strategies have stronger exploration ability compared to the heuristic rule-based methods. However, it should be noted that GFlowDA can achieve better performance and exploration than RLADA. This is because RLADA tends to explore near the maximum reward, while GFlowDA explores according to the reward distribution.

Transferability of GFlowDA on GUDA. The active pol-

Table 4: Comparison results on more settings and methods.

Method	Office3	1-Origin	OH-F	RUST	Office3	1-GUDA	OH-GUDA		
memou	Acc	JSD	Acc	JSD	Acc	JSD	Acc	JSD	
AUDA	90.43	16.32	59.43	14.85	66.53	17.35	50.35	12.10	
LAMDA	89.91	15.97	61.26	13.07	70.02	14.84	<u>53.86</u>	11.37	
GFlowDA	92.85	15.67	63.19	11.34	74.86	9.68	61.40	5.65	

icy network of GFlowDA is capable of effectively transferring to tasks with varying degrees of label distribution shift and label space mismatch. To prove this, we adjust the degree of label heterogeneity by controlling the JSD distance between the source and target label distribution, denoted as $d_{\rm JS}(P_s^Y,P_t^Y)$. As this distance increases, DA tasks become more challenging. Fig. I represents the transferability of our method compared with existing ADA methods in $A\rightarrow W$ on Office-31 (More results are available in the appendix). The term "GFlowDA" refers to directly loading the active policy network pre-trained on the original dataset. "GFlowDA trained" indicates that the policy model has been fine-tuned on the new tasks by training 30 epochs. Our experimental results demonstrate that GFlowDA can directly transfer to new tasks without training, and outperforms non-learning based methods in most cases. Furthermore, 'GFlowDA trained" improves performance on specific tasks

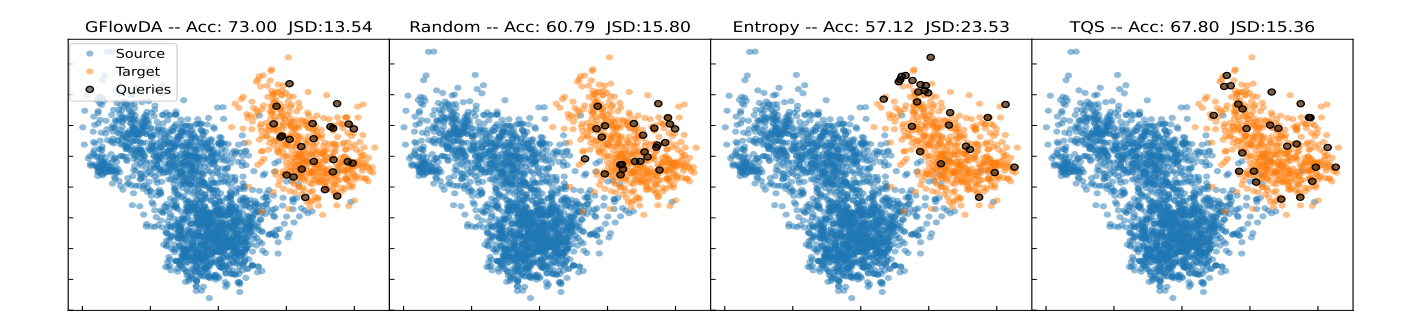


Figure 5: Feature visualization on the Office-31 A \rightarrow W task. Selected samples are shown as black dots in the plots.

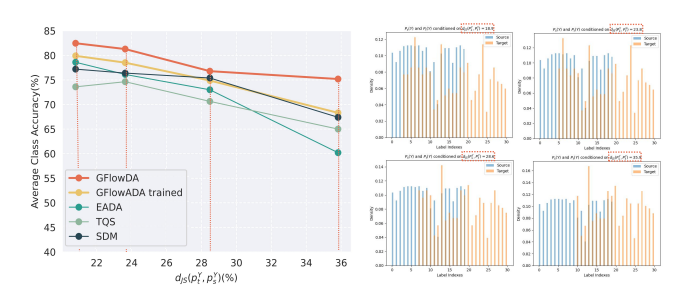


Figure 6: **Left**: Accuracy with varying $d_{\rm JS}(P_s^Y,P_t^Y)$ values. **Right**: Label distribution with varying $d_{\rm JS}(P_s^Y,P_t^Y)$ values.

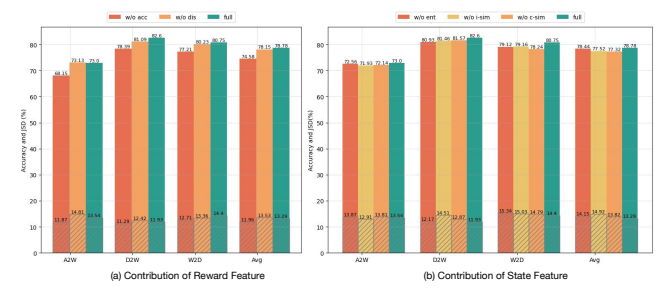


Figure 7: Ablation Study. "dis" indicates MMD. "i-sim" and "c-sim" indicate instance and class-level similarity.

compared to 'GFlowDA'. The transfer of active learning strategies is practically challenging, making the advantages of our method even more apparent and highlighting its strong transferability.

5.3. Further Analysis of GFlowDA

Performance of GFlowDA on Existing Settings. To demonstrate the effectiveness of GFlowDA in handling the variants included in GUDA, we evaluated its performance on Office31-Origin and OfficeHome-RUST. The former represents the original setting without any manual modification, while the latter represents the GLS scenario [16]. As shown in Table 4, our method outperforms or achieves comparable results to methods specifically designed for these variants. This highlights the robustness of our approach and its ability to adapt to different domain adaptation settings.

Performance of Existing methods on GUDA. Due to the absence of active learning in previous label space mismatch and label distribution shift methods, as well as differences in prediction space ($|\hat{\mathcal{Y}}| = k+1$), it is unfair and impractical to directly compare GFlowDA with those methods. To ensure fairness and gain a deeper understanding of GFlowDA, we analyze AUDA and LAMDA separately, which are active learning methods developed for the UniDA and GLS settings respectively. As shown in the Tbale 4, their performance significantly decreases when applied to the GUDA setting. This fully demonstrates that GUDA is

a more realistic and complex scenario and can guide us in proposing GFlowDA for solving all the variants.

Qualitative Analysis As illustrated in Fig. 5, we present the feature visualization on Office-31 A \rightarrow W with 5% budget. It is obvious that the samples selected by GFlowDA can effectively restore the target label distribution, thus contributing to addressing GUDA problems. In comparison, the Random method provides a certain level of estimation for the target distribution compared to Entropy, it lacks stability and does not consider sample informativeness. The Entropy and TQS methods prioritize prediction uncertainty in sample selection, resulting in the inclusion of distant samples from the source domain. Consequently, these methods may not fully restore the target label distribution, leading to suboptimal performance.

Varying the Label Budget. To demonstrate the effectiveness of GFlowDA, we conducted experiments with varying the labeling budget from 0% to 10%, as shown in Figure 4. Across both Office-31 and Office-Home datasets, GFlowDA consistently outperforms baselines in terms of accuracy and JSD, showcasing GFlowDA can provide excellent performance across varying labeling budgets, making it a promising solution to address GUDA.

5.4. Ablation Study of GFlowDA

Contribution of State Features. We further investigate the impact of the state features introduced in Section 4.2.

To study how each feature affects the learned policy, we remove them from the state space individually and examine the resulting performance. The experimental results are illustrated in Figure 7 (b), which shows the performance of GFlowDA with three variants of the state on Office-31. It can be observed that removing any of the features can result in a drop in accuracy, implying that each feature plays a crucial role in achieving the high performance of GFlowDA.

Contribution of Reward Features. In addition to examining the state features, we further analyzed the effectiveness of different variants of reward on GFlowDA's performance. Figure 7 (a) shows the results of this experiment. We found that the impact of reward on GFlowDA's performance is relatively significant compared to state features. Ignoring either component would lead to a passive impact on the overall performance of GFlowDA. While accuracy makes the selection of samples more informative, MMD allows the chosen samples to better explore the target distribution. Overall, our analysis suggests that the unique combination of state design and reward mechanism can effectively address GUDA.

6. Conclusion

In this work, we propose a comprehensive problem GUDA, which aims to obtain accurate predictions for unknown categories while addressing label heterogeneity. We develop an active learning domain adaptation method, GFlowDA, by leveraging GFlowNets' exploration capabilities. To achieve this, we propose a design paradigm of state and reward, along with an efficient solution for parent exploration and state transition. Additionally, GFlowDA introduces a training framework named GUAN for GUDA. Experimental results demonstrate GFlowDA's superior performance over other SOTA methods in five benchmarks.

References

- [1] Mahsa Baktashmotlagh, Masoud Faraki, Tom Drummond, and Mathieu Salzmann. Learning factorized representations for open-set domain adaptation. *arXiv preprint arXiv:1805.12277*, 2018. 2
- [2] Shai Ben-David, John Blitzer, Koby Crammer, Alex Kulesza, Fernando Pereira, and Jennifer Wortman Vaughan. A theory of learning from different domains. *Machine learning*, 79(1):151–175, 2010.
- [3] Emmanuel Bengio, Moksh Jain, Maksym Korablyov, Doina Precup, and Yoshua Bengio. Flow network based generative models for non-iterative diverse candidate generation. *Advances in Neural Information Processing Systems*, 34:27381–27394, 2021. 2, 3, 16
- [4] Yoshua Bengio, Tristan Deleu, Edward J Hu, Salem Lahlou, Mo Tiwari, and Emmanuel Bengio. Gflownet foundations. *arXiv preprint arXiv:2111.09266*, 2021. 3, 4, 14, 15
- [5] Zhangjie Cao, Mingsheng Long, Jianmin Wang, and Michael I Jordan. Partial transfer learning with selective adversarial networks. In *Proceedings of the IEEE conference on*

- computer vision and pattern recognition, pages 2724–2732, 2018. 3
- [6] Antoine de Mathelin, François Deheeger, Mathilde Mougeot, and Nicolas Vayatis. Discrepancy-based active learning for domain adaptation. In *International Conference on Learning Representations*, 2021. 2, 3
- [7] Jia Deng. A large-scale hierarchical image database. Proc. of IEEE Computer Vision and Pattern Recognition, 2009, 2009.
- [8] Lixin Duan, Ivor W Tsang, and Dong Xu. Domain transfer multiple kernel learning. *IEEE Transactions on Pattern Analysis and Machine Intelligence*, 34(3):465–479, 2012. 1
- [9] Bo Fu, Zhangjie Cao, Mingsheng Long, and Jianmin Wang. Learning to detect open classes for universal domain adaptation. In *European Conference on Computer Vision*, pages 567–583. Springer, 2020. 2, 16, 17
- [10] Bo Fu, Zhangjie Cao, Jianmin Wang, and Mingsheng Long. Transferable query selection for active domain adaptation. In *Proceedings of the IEEE/CVF Conference on Computer Vision and Pattern Recognition*, pages 7272–7281, 2021. 2, 3, 7, 8, 16, 17
- [11] Yaroslav Ganin, Evgeniya Ustinova, Hana Ajakan, Pascal Germain, Hugo Larochelle, François Laviolette, Mario Marchand, and Victor Lempitsky. Domain-adversarial training of neural networks. *The journal of machine learning research*, 17(1):2096–2030, 2016.
- [12] Saurabh Garg, Sivaraman Balakrishnan, and Zachary C Lipton. Domain adaptation under open set label shift. arXiv preprint arXiv:2207.13048, 2022. 3
- [13] Kaiming He, Xiangyu Zhang, Shaoqing Ren, and Jian Sun. Deep residual learning for image recognition. In *Proceedings of the IEEE conference on computer vision and pattern recognition*, pages 770–778, 2016. 1, 18
- [14] Judy Hoffman, Eric Tzeng, Taesung Park, Jun-Yan Zhu, Phillip Isola, Kate Saenko, Alexei Efros, and Trevor Darrell. Cycada: Cycle-consistent adversarial domain adaptation. In *International conference on machine learning*, pages 1989– 1998. PMLR, 2018. 1, 2
- [15] Lanqing Hu, Meina Kan, Shiguang Shan, and Xilin Chen. Duplex generative adversarial network for unsupervised domain adaptation. In *Proceedings of the IEEE Conference on Computer Vision and Pattern Recognition*, pages 1498–1507, 2018.
- [16] Sehyun Hwang, Sohyun Lee, Sungyeon Kim, Jungseul Ok, and Suha Kwak. Combating label distribution shift for active domain adaptation. In *European Conference on Computer Vision*, pages 549–566. Springer, 2022. 2, 3, 7, 8, 9, 16, 17
- [17] Moksh Jain, Emmanuel Bengio, Alex Hernandez-Garcia, Jarrid Rector-Brooks, Bonaventure FP Dossou, Chanakya Ajit Ekbote, Jie Fu, Tianyu Zhang, Michael Kilgour, Dinghuai Zhang, et al. Biological sequence design with gflownets. In *International Conference on Machine Learning*, pages 9786–9801. PMLR, 2022. 3
- [18] Guoliang Kang, Liang Zheng, Yan Yan, and Yi Yang. Deep adversarial attention alignment for unsupervised domain adaptation: the benefit of target expectation maximization. In *Proceedings of the European conference on computer vision* (ECCV), pages 401–416, 2018.

- [19] Matthieu Kirchmeyer, Alain Rakotomamonjy, Emmanuel de Bezenac, and Patrick Gallinari. Mapping conditional distributions for domain adaptation under generalized target shift. arXiv preprint arXiv:2110.15057, 2021. 2
- [20] Alex Krizhevsky, Ilya Sutskever, and Geoffrey E Hinton. Imagenet classification with deep convolutional neural networks. Advances in neural information processing systems, 25, 2012.

 1, 18
- [21] Trung Le, Tuan Nguyen, Nhat Ho, Hung Bui, and Dinh Phung. Lamda: Label matching deep domain adaptation. In *International Conference on Machine Learning*, pages 6043–6054. PMLR, 2021. 2
- [22] Da Li, Yongxin Yang, Yi-Zhe Song, and Timothy M Hospedales. Deeper, broader and artier domain generalization. In *Proceedings of the IEEE international conference on* computer vision, pages 5542–5550, 2017. 7, 16
- [23] Guangrui Li, Guoliang Kang, Yi Zhu, Yunchao Wei, and Yi Yang. Domain consensus clustering for universal domain adaptation. In *Proceedings of the IEEE/CVF Conference on Computer Vision and Pattern Recognition*, pages 9757–9766, 2021. 2
- [24] Wenqian Li, Yinchuan Li, Zhigang Li, Jianye Hao, and Yan Pang. Dag matters! gflownets enhanced explainer for graph neural networks. arXiv preprint arXiv:2303.02448, 2023. 3
- [25] Jian Liang, Yunbo Wang, Dapeng Hu, Ran He, and Jiashi Feng. A balanced and uncertainty-aware approach for partial domain adaptation. In *European Conference on Computer Vision*, pages 123–140. Springer, 2020. 3
- [26] Omri Lifshitz and Lior Wolf. A sample selection approach for universal domain adaptation. arXiv preprint arXiv:2001.05071, 2020. 2
- [27] Mingsheng Long, Yue Cao, Jianmin Wang, and Michael Jordan. Learning transferable features with deep adaptation networks. In *International conference on machine learning*, pages 97–105. PMLR, 2015. 1
- [28] Mingsheng Long, Han Zhu, Jianmin Wang, and Michael I Jordan. Deep transfer learning with joint adaptation networks. In Proceedings of the 34th International Conference on Machine Learning-Volume 70, pages 2208–2217. JMLR, 2017.
- [29] Xinhong Ma, Junyu Gao, and Changsheng Xu. Active universal domain adaptation. In *Proceedings of the IEEE/CVF International Conference on Computer Vision*, pages 8968–8977, 2021. 2, 3
- [30] Nikolay Malkin, Moksh Jain, Emmanuel Bengio, Chen Sun, and Yoshua Bengio. Trajectory balance: Improved credit assignment in gflownets. arXiv preprint arXiv:2201.13259, 2022. 3
- [31] Pau Panareda Busto and Juergen Gall. Open set domain adaptation. In *Proceedings of the IEEE international conference on computer vision*, pages 754–763, 2017. 2
- [32] Xingchao Peng, Qinxun Bai, Xide Xia, Zijun Huang, Kate Saenko, and Bo Wang. Moment matching for multi-source domain adaptation. In *Proceedings of the IEEE/CVF international conference on computer vision*, pages 1406–1415, 2019. 7, 16
- [33] Xingchao Peng, Ben Usman, Neela Kaushik, Dequan Wang, Judy Hoffman, and Kate Saenko. Visda: A synthetic-to-real

- benchmark for visual domain adaptation. In *Proceedings* of the IEEE Conference on Computer Vision and Pattern Recognition Workshops, pages 2021–2026, 2018. 7, 16
- [34] Viraj Prabhu, Arjun Chandrasekaran, Kate Saenko, and Judy Hoffman. Active domain adaptation via clustering uncertainty-weighted embeddings. In *Proceedings of the IEEE/CVF International Conference on Computer Vision*, pages 8505–8514, 2021. 2, 3, 7, 16, 17
- [35] Piyush Rai, Avishek Saha, Hal Daumé III, and Suresh Venkatasubramanian. Domain adaptation meets active learning. In *Proceedings of the NAACL HLT 2010 Workshop on Active Learning for Natural Language Processing*, pages 27– 32, 2010. 3
- [36] Alain Rakotomamonjy, Rémi Flamary, Gilles Gasso, M El Alaya, Maxime Berar, and Nicolas Courty. Optimal transport for conditional domain matching and label shift. *Machine Learning*, 111(5):1651–1670, 2022.
- [37] Kate Saenko, Brian Kulis, Mario Fritz, and Trevor Darrell. Adapting visual category models to new domains. In European conference on computer vision, pages 213–226. Springer, 2010. 1, 7, 16
- [38] Kuniaki Saito, Donghyun Kim, Stan Sclaroff, and Kate Saenko. Universal domain adaptation through self supervision. Advances in neural information processing systems, 33:16282–16292, 2020. 2
- [39] Kuniaki Saito and Kate Saenko. Ovanet: One-vs-all network for universal domain adaptation. In *Proceedings of the IEEE/CVF International Conference on Computer Vision*, pages 9000–9009, 2021. 2
- [40] Kuniaki Saito, Kohei Watanabe, Yoshitaka Ushiku, and Tatsuya Harada. Maximum classifier discrepancy for unsupervised domain adaptation. In *Proceedings of the IEEE con*ference on computer vision and pattern recognition, pages 3723–3732, 2018. 2
- [41] Kuniaki Saito, Shohei Yamamoto, Yoshitaka Ushiku, and Tatsuya Harada. Open set domain adaptation by backpropagation. In Proceedings of the European Conference on Computer Vision (ECCV), pages 153–168, 2018. 1, 2
- [42] John Schulman, Filip Wolski, Prafulla Dhariwal, Alec Radford, and Oleg Klimov. Proximal policy optimization algorithms. arXiv preprint arXiv:1707.06347, 2017. 7, 18
- [43] Changjian Shui, Zijian Li, Jiaqi Li, Christian Gagné, Charles X Ling, and Boyu Wang. Aggregating from multiple target-shifted sources. In *International Conference on Machine Learning*, pages 9638–9648. PMLR, 2021. 2
- [44] Karen Simonyan and Andrew Zisserman. Very deep convolutional networks for large-scale image recognition. *arXiv* preprint arXiv:1409.1556, 2014. 1
- [45] Jong-Chyi Su, Yi-Hsuan Tsai, Kihyuk Sohn, Buyu Liu, Subhransu Maji, and Manmohan Chandraker. Active adversarial domain adaptation. In *Proceedings of the IEEE/CVF Winter Conference on Applications of Computer Vision*, pages 739–748, 2020. 3
- [46] Richard S Sutton and Andrew G Barto. *Reinforcement learning: An introduction*. MIT press, 2018. 3
- [47] Remi Tachet des Combes, Han Zhao, Yu-Xiang Wang, and Geoffrey J Gordon. Domain adaptation with conditional

- distribution matching and generalized label shift. *Advances in Neural Information Processing Systems*, 33:19276–19289, 2020. 2, 3, 4, 7, 13, 16
- [48] Eric Tzeng, Judy Hoffman, Kate Saenko, and Trevor Darrell. Adversarial discriminative domain adaptation. In *Proceedings of the IEEE conference on computer vision and pattern recognition*, pages 7167–7176, 2017.
- [49] Hemanth Venkateswara, Jose Eusebio, Shayok Chakraborty, and Sethuraman Panchanathan. Deep hashing network for unsupervised domain adaptation. In *Proceedings of the IEEE* conference on computer vision and pattern recognition, pages 5018–5027, 2017. 7, 16
- [50] Dan Wang and Yi Shang. A new active labeling method for deep learning. In 2014 International joint conference on neural networks (IJCNN), pages 112–119. IEEE, 2014. 7, 8, 16, 17
- [51] Xuezhi Wang and Jeff Schneider. Flexible transfer learning under support and model shift. Advances in Neural Information Processing Systems, 27, 2014. 1, 16
- [52] Binhui Xie, Longhui Yuan, Shuang Li, Chi Harold Liu, Xinjing Cheng, and Guoren Wang. Active learning for domain adaptation: An energy-based approach. In *Proceedings of the AAAI Conference on Artificial Intelligence*, volume 36, pages 8708–8716, 2022. 2, 3, 7, 8, 16, 17
- [53] Ming Xie, Yuxi Li, Yabiao Wang, Zekun Luo, Zhenye Gan, Zhongyi Sun, Mingmin Chi, Chengjie Wang, and Pei Wang. Learning distinctive margin toward active domain adaptation. In *Proceedings of the IEEE/CVF Conference on Computer Vision and Pattern Recognition*, pages 7993–8002, 2022. 2, 3, 7, 8, 16, 17
- [54] Kaichao You, Mingsheng Long, Zhangjie Cao, Jianmin Wang, and Michael I Jordan. Universal domain adaptation. In *Proceedings of the IEEE/CVF conference on computer vision and pattern recognition*, pages 2720–2729, 2019. 1, 2, 7, 16
- [55] Dinghuai Zhang, Nikolay Malkin, Zhen Liu, Alexandra Volokhova, Aaron Courville, and Yoshua Bengio. Generative flow networks for discrete probabilistic modeling. arXiv preprint arXiv:2202.01361, 2022. 3
- [56] Jing Zhang, Zewei Ding, Wanqing Li, and Philip Ogunbona. Importance weighted adversarial nets for partial domain adaptation. In *Proceedings of the IEEE conference on computer vision and pattern recognition*, pages 8156–8164, 2018. 1, 3
- [57] Kun Zhang, Bernhard Schölkopf, Krikamol Muandet, and Zhikun Wang. Domain adaptation under target and conditional shift. In *International Conference on Machine Learn*ing, pages 819–827. PMLR, 2013. 1
- [58] Han Zhao, Remi Tachet Des Combes, Kun Zhang, and Geoffrey Gordon. On learning invariant representations for domain adaptation. In *International Conference on Machine Learning*, pages 7523–7532. PMLR, 2019. 2

A. Preliminaries

To increase the readability of this paper, we provide a summary of the important notations used throughout this work in Table E. In order to make a more effective comparison between GUDA and its sub-problems, we give the formal problem settings and further analysis for the tasks of LS, GLS, PDA, OSDA and UniDA. In the tasks of LS, GLS and PDA, there is no private label space in the target domain, which means $\mathcal{Y}_t = \mathcal{Y}_c$. The target risk of these tasks can be expressed as:

$$\epsilon_{t}(h \circ g) = \mathbb{E}_{(X,Y) \sim \mathcal{D}_{t}} \ell(h \circ g(X), Y)$$

$$= \underbrace{\sum_{i=1}^{k} P_{t}(Y = i) \epsilon_{t,i}(h \circ g)}_{\text{target common risk}},$$
 (s)

where $\epsilon_{t,i}(h \circ g) = \mathbb{E}_{X \sim P_t(X|Y=i)} \ell(h \circ g(X), i)$ denotes the expected loss of applying the classifier $h \circ g$ to an input variable X, which is drawn from the conditional distribution $P_t(X \mid Y = i)$ and compared with the true label i by the loss function $\ell(\cdot)$.

In the tasks of UniDA and OSDA, all target private classes are recognized as a single class. The target label space can be expressed as $\mathcal{Y}_t = \{\mathcal{Y}_c, \text{unk}\} = \{1, 2, \dots, k, k + 1\}$ 1}, including an additional unknown class labeled k+1. The target risk of these tasks can be decomposed into two components: the target common risk for classifying common classes and the target private risk for grouping all private classes into the k + 1-th class:

$$\epsilon_{t}(h \circ g) = \mathbb{E}_{(X,Y) \sim \mathcal{D}_{t}} \ell(h \circ g(X), Y) \qquad \text{(t)} \qquad \text{classifier } \widehat{Y} = (h \circ g)(X),$$

$$= \underbrace{\sum_{i=1}^{k} P_{t}(Y = i) \epsilon_{t,i}(h \circ g)}_{\text{target common risk}} + \underbrace{P_{t}(Y = k+1) \epsilon_{t,k+1}(h \circ g),}_{\text{target private risk}} \quad |\epsilon_{s}(h \circ g) - \epsilon_{t}(h \circ g)| \\ \leq \|P_{s}(Y) - P_{t}(Y)\|_{1} \cdot \varepsilon_{s}(\widehat{Y}\|Y) + 2(k-1)\Delta_{s,t}(\widehat{Y}\|Y).$$

This subsection primarily aims to introduce the target risks of these tasks, which can be classified into two cases, i.e., Eq. s and Eq. t, depending on the existence of a target private label set.

B. Proof of Theorem 1

Theorem 2 (Target Risk Upper Bound for GUDA). Let Y_c , Y_l and \overline{Y}_t be random variables taking values from \mathcal{Y}_c , \mathcal{Y}_l and $\overline{\mathcal{Y}}_t$ respectively, with \mathcal{Y}_l being the selected target label space. For any classifier $\hat{Y} = (h \circ g)(X)$, we have

$$\epsilon_t(h \circ g) \le \epsilon_s(h \circ g) + \epsilon_l(h \circ g) + \delta_{s,t} + \delta_{l,t} + \varepsilon_t(\widehat{Y}||\overline{Y}_t),$$
where

$$\delta_{s,t} = \|P_s(Y_c) - P_t(Y_c)\|_1 \cdot \varepsilon_s(\widehat{Y}||Y_c) + 2(k-1)\Delta_{s,t}(\widehat{Y}||Y_c)$$

$$\delta_{l,t} = \|P_l(Y_l) - P_t(Y_l)\|_1 \cdot \varepsilon_l(\widehat{Y}||Y_l) + 2(v-1)\Delta_{l,t}(\widehat{Y}||Y_l)$$

Table E: Important notations in this paper.

Notation	Meaning
b	Labeling budget
s_t	State of GFlowDA at step t
a_t	Action of GFlowDA at step t
$r(\cdot)$	Reward function of GFlowDA
$\pi(\cdot)$	Active generative policy network
$h(\cdot)$	Label classification function
$g(\cdot)$	Feature transformation function
$\varepsilon(\cdot)$	Error Function
X	Random variables of input space
Y	Random variables of label space
\widehat{Y}	The prediction result of $h \circ g(X)$
Z	Random variables of latent space
$P_{\mathcal{S}}$	Source distribution
P_t	Target distribution
$\mathcal{D}_{\mathcal{S}}^{\circ}$	Labeled source dataset
\mathcal{D}_t	Unlabeled target dataset
\mathcal{D}_{l}°	Queried target dataset

with k being the common label set size and $v = |\mathcal{Y}_l|$ being the selected label set size, $||P_s(Y_c) - P_t(Y_c)||_1 =$ $\sum_{i \in \mathcal{Y}_c} |P_s(Y=i) - P_t(Y=i)|$ being the L_1 distance between $P_s(Y)$ and $P_t(Y)$ on the common label space \mathcal{Y}_c .

Before we give the proof of Theorem 2, we first present the error decomposition theorem proposed by [47] under the assumption that $\mathcal{Y}_s = \mathcal{Y}_t$, which is stated as follows.

Theorem 3 (Error Decomposition Theorem [47]). For any classifier $\widehat{Y} = (h \circ q)(X)$,

$$\begin{aligned} &|\epsilon_s(h \circ g) - \epsilon_t(h \circ g)| \\ &\leq &\|P_s(Y) - P_t(Y)\|_1 \cdot \varepsilon_s(\widehat{Y} \| Y) + 2(k-1)\Delta_{s,t}(\widehat{Y} \| Y) \end{aligned}$$

Proof of Theorem 2. Followed by [47], we denote $\gamma_{s,j} =$ $P_s(Y=j)$ for simplicity. The following identity holds for $a \in \{s, l, t\}$ by the law of total probability:

$$\epsilon_{a}(h \circ g) = \mathbb{E}_{(X,Y) \sim P_{a}} \ell(h \circ g(X), Y)$$

$$= \mathbb{E}_{(X,Y) \sim P_{a}} P_{a}(\widehat{Y} \neq Y)$$

$$= \sum_{i \neq j} P_{a}(\widehat{Y} = i, Y = j)$$

$$= \sum_{i \neq j} \gamma_{a,j} P_{a}(\widehat{Y} = i \mid Y = j).$$

We further decompose the target risk $\epsilon_t(h \circ q)$ and the source risk $\epsilon_s(h \circ g)$ based on their common and private label space. Then we have:

$$\begin{split} &\epsilon_{t}(h \circ g) - \epsilon_{s}(h \circ g) \\ &= \mathbb{E}_{(X,Y) \sim \mathcal{D}_{t}} P_{t}(Y \neq \widehat{Y}) - \mathbb{E}_{(X,Y) \sim \mathcal{D}_{s}} P_{s}(Y \neq \widehat{Y}) \\ &= \sum_{i \neq j} \gamma_{t,j} P_{t}(i|j) - \sum_{i \neq j} \gamma_{s,j} P_{s}(i|j) \\ &= \sum_{i \neq j,j \in \mathcal{Y}_{c}} \gamma_{t,j} P_{t}(i|j) - \sum_{i \neq j,j \in \mathcal{Y}_{c}} \gamma_{s,j} P_{s}(i|j) \\ &+ \sum_{i \neq j,j \in \overline{\mathcal{Y}}_{t}} \gamma_{t,j} P_{t}(i|j) - \sum_{i \neq j,j \in \overline{\mathcal{Y}}_{s}} \gamma_{s,j} P_{s}(i|j) \\ &\leq \left| \sum_{i \neq j,j \in \mathcal{Y}} \gamma_{t,j} P_{t}(i|j) - \sum_{i \neq j,j \in \mathcal{Y}_{s}} \gamma_{s,j} P_{s}(i|j) \right| \\ &+ \sum_{i \neq j,j \in \overline{\mathcal{Y}}_{t}} \gamma_{t,j} P_{t}(i|j) - \sum_{i \neq j,j \in \overline{\mathcal{Y}}_{s}} \gamma_{s,j} P_{s}(i|j). \end{split}$$

where $P_t(i|j)$ indicates $P_t(\widehat{Y} = i|Y = j)$ for simplicity. Based on Theorem 3, we can obtain:

$$\begin{split} & \left| \sum_{i \neq j, j \in \mathcal{Y}_c} \gamma_{t,j} P_t(i|j) - \sum_{i \neq j, j \in \mathcal{Y}_c} \gamma_{s,j} P_s(i|j) \right| \\ \leq & \| P_s(Y_c) - P_t(Y_c) \|_1 \cdot \varepsilon_s(\widehat{Y} \| Y_c) + 2(k-1) \Delta_{s,t}(\widehat{Y} \| Y_c), \end{split}$$

Using the above inequality, we have:

$$\mathbb{E}_{(X,Y)\sim\mathcal{D}_{t}}P_{t}(Y\neq\widehat{Y}) - \mathbb{E}_{(X,Y)\sim\mathcal{D}_{s}}P_{s}(Y\neq\widehat{Y})$$

$$\leq \|P_{s}(Y_{c}) - P_{t}(Y_{c})\|_{1} \cdot \varepsilon_{s}(\widehat{Y}\|Y_{c}) + 2(k-1)\Delta_{s,t}(\widehat{Y}\|Y_{c})$$

$$+ \sum_{i\neq j,j\in\overline{\mathcal{Y}}_{t}} \gamma_{t,j}P_{t}(i|j) - \sum_{i\neq j,j\in\overline{\mathcal{Y}}_{s}} \gamma_{s,j}P_{s}(i|j).$$

Recall that the source risk can be decomposed into two parts:

$$\mathbb{E}_{(X,Y)\sim\mathcal{D}_s} P_s(Y \neq \widehat{Y}) = \sum_{i \neq j, j \in \overline{\mathcal{Y}}_s} \gamma_{s,j} P_s(i|j) + \sum_{i \neq j, j \in \mathcal{Y}_c} \gamma_{s,j} P_s(i|j).$$

Combining the above inequality and identity, we have:

$$\mathbb{E}_{(X,Y)\sim\mathcal{D}_{t}}P_{t}(Y\neq\widehat{Y})$$

$$\leq \|P_{s}(Y) - P_{t}(Y)\|_{1} \cdot \varepsilon_{s}(\widehat{Y}\|Y) + 2(k-1)\Delta_{s,t}(\widehat{Y}\|Y)$$

$$+ \sum_{i\neq j,j\in\overline{\mathcal{Y}}_{t}} \gamma_{t,j}P_{t}(i|j) + \sum_{i\neq j,j\in\mathcal{Y}_{c}} \gamma_{s,j}P_{s}(i|j).$$

For simplicity, we still use $\epsilon_s(h \circ g)$ to denote the classification error on common label space, i.e., the last term of the above inequality. We have:

$$\begin{split} & \epsilon_t(h \circ g) \leq \epsilon_s(h \circ g) \\ & + \|P_s(Y) - P_t(Y)\|_1 \cdot \varepsilon_s(\widehat{Y} \| Y) + 2(k-1)\Delta_{s,t}(\widehat{Y} \| Y) \\ & + \sum_{i \neq j, j \in \overline{\mathcal{Y}}_T} \gamma_{t,j} P_t(i|j). \end{split}$$

Moreover, we have

$$\sum_{i \neq j, j \in \overline{\mathcal{Y}}_T} \gamma_{t,j} P_t(i|j) \le \varepsilon_t(\widehat{Y}||\overline{Y}_t),$$

where

$$\varepsilon_t(\widehat{Y}||\overline{Y}_t) := \max_{j \in \overline{\mathcal{Y}}_t} P_s(\widehat{Y} \neq Y \mid Y = j),$$

and hence,

$$\epsilon_{t}(h \circ g) \leq \epsilon_{s}(h \circ g)$$

$$+ \|P_{s}(Y) - P_{t}(Y)\|_{1} \cdot \varepsilon_{s}(\widehat{Y} \| Y) + 2(k-1)\Delta_{s,t}(\widehat{Y} \| Y)$$

$$+ \varepsilon_{t}(\widehat{Y} \| \overline{Y}_{t}).$$

It is worth noting that the above target upper bound only involves the source domain \mathcal{D}_s . Since active learning is required in GUDA, an additional domain \mathcal{D}_l corresponding to the selecting labeled target data is introduced. Similar to the above inequality, for the error decomposition between the target and the selected labeled target domain, we have:

$$\epsilon_{t}(h \circ g) \leq \epsilon_{l}(h \circ g)$$

$$+ \|P_{l}(Y_{l}) - P_{t}(Y_{l})\|_{1} \cdot \varepsilon_{l}(\widehat{Y} \| Y_{l}) + 2(v - 1)\Delta_{l,t}(\widehat{Y} \| Y_{l})$$

$$+ \varepsilon_{t}(\widehat{Y} \| \overline{Y}_{t}).$$

Note that the common label space between the selected target domain \mathcal{D}_l and the original target domain \mathcal{D}_t is \mathcal{Y}_l due to $\mathcal{Y}_l \subseteq \mathcal{Y}_t$. Finally, combining the above two inequalities, we get:

$$\epsilon_t(h \circ g) \le \epsilon_s(h \circ g) + \epsilon_l(h \circ g) + \delta_{s,t} + \delta_{l,t} + \varepsilon_t(\widehat{Y}||\overline{Y}_t),$$

where

$$\delta_{s,t} = \|P_s(Y_c) - P_t(Y_c)\|_1 \cdot \varepsilon_s(\widehat{Y}||Y_c) + 2(k-1)\Delta_{s,t}(\widehat{Y}||Y_c) \delta_{l,t} = \|P_l(Y_l) - P_t(Y_l)\|_1 \cdot \varepsilon_l(\widehat{Y}||Y_l) + 2(v-1)\Delta_{l,t}(\widehat{Y}||Y_l).$$

Above all, we complete the proof of Theorem 2.

C. More Flow Modeling Details

For clarity, we present details about flow modeling in GFlowNet[4] here. Given a directed acyclic graph (DAG) with state and action sets $(\mathcal{S},\mathcal{A})$ as illustrated in Fig H, in which there is no trajectory $(s_0,s_1,...,s_f)$ satisfying $s_i=s_j, \forall i\neq j$. Define s_0 and s_f respectively as the initial state and the final state, then a *complete trajectory* is defined as a sequence of states $\tau=(s_0,...,s_f)$. Then we can define the concept of flow as follows.

Definition 8 (Edge Flow [4]). An edge flow $F(s_t \rightarrow s_{t+1}) \mapsto \mathbb{R}$ is the flow through an edge $s_t \rightarrow s_{t+1}$.

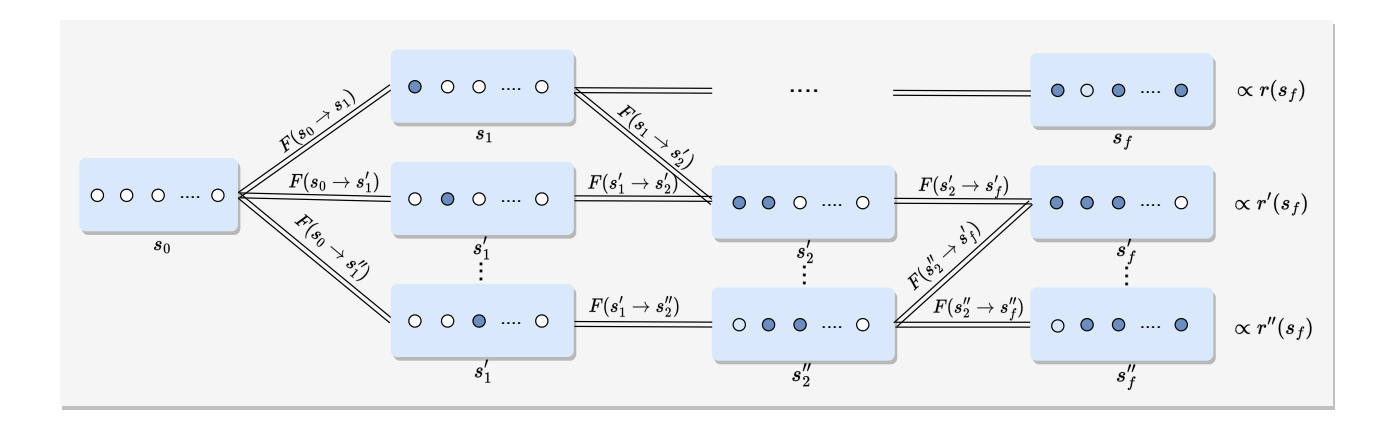


Figure H: DAG Structure of GFlowDA. The DAG \mathcal{G} operates analogously as a water pipe, where water enters at s_0 and flows out through all s_f , satisfying the condition $F(s_0) = \sum F(s_f) = \sum F(s_f)$.

Algorithm 1 GFlowDA: Generative Flow Domain Adaptation

Input:

1: \mathcal{D}_s : Labeled source dataset; \mathcal{D}_t : Unlabeled target dataset; \mathcal{D}_l : Selected labeled target dataset; b: Labeling budget; E: Epoch number; η : Learning rate; h: Label classifier; h: Feature extractor; $\pi(\theta)$: Active generative policy.

2: repeat

- 3: Pretrain h and g based on \mathcal{D}_s and \mathcal{D}_t via Eq.15 and Eq.18
- 4: Initialize $\mathcal{D}_l = \emptyset$
- 5: repeat
- 6: Computing s_t according to Eq.4, Eq.5, Eq.7 and Eq.8
- 7: Sample a valid action $a_t = i$ by the active generative policy $\pi(s_t)$
- 8: Annotate the corresponding target sample x_i by y_i
- 9: Update the selected labeled target dataset $\mathcal{D}_l = \mathcal{D}_l \cup \{x_i, y_i\}$
- 10: **until** The labeling budget b is used up
- 11: Update the domain adaptation model h and g using \mathcal{D}_l via Eq.15, Eq.16 and Eq.18
- 12: Compute reward $r(s_f)$ on terminal state s_f from each trajectory via Eq.9
- 13: Update $\pi(\theta)$ w.r.t. the objective in Eq.14 for all trajectories in the minibatch
- 14: **until** epoch number E is reached

Output: $\pi(\theta)$

Definition 9 (Trajectory Flow [4]). Given a complete trajectory $\tau \in \mathcal{T}$, the corresponding trajectory flow $F(\tau) : \tau \mapsto \mathbb{R}^+$ is defined as any non-negative function defined on \mathcal{T} , which contains the number of particles sharing the same

path τ .

Definition 10 (State Flow [4]). For any state $s \in \mathcal{S}$, the corresponding state flow $F(s): \mathcal{S} \mapsto \mathbb{R}$ is the sum of the flows of the complete trajectories passing through it, i.e., $F(s) = \sum_{\tau \in \tau} \mathbb{1}_{s \in \tau} F(\tau)$.

Definition 11 (Action Flow [4]). The action flow $F(s_t, a_t)$: $S \times A \mapsto \mathbb{R}$ is the flow of the complete trajectory passing through state s_t with a specific action a_t . When $a_t : s_t \to s_{t+1}$, $F(s_t, a_t)$ is equal to the edge flow $F(s_t \to s_{t+1})$.

Introducing this flow model is critical to establishing a policy that could sample exactly proportional to rewards. We can imagine the DAG structure as a water pipe, where the total inflows equal the total outflows (rewards). In this way, total rewards can be distributed to different nodes, and the probability of each action can be easily measured by the fraction of action flow F(s,a) to state flow F(s), making it possible to achieve precise proportionality between final policies and rewards.

Definition 12 (Transition Probability [4]). For a non-negative flow function $F(\cdot)$, the corresponding forward transition probability $\pi_F(s_t \to s_{t+1}|s_t)$ is a special case of conditional probability:

$$\pi_F(s_{t+1}|s_t) := \pi_F(s_t \to s_{t+1}|s_t) = \frac{F(s_t \to s_{t+1})}{F(s_t)}.$$
 (u)

Then, we have $\pi_F(\tau) = \prod_{t=0}^{f-1} \pi_F(s_{t+1}|s_t)$, which yields

$$\pi_F(s_f) = \frac{\sum_{\tau \in \mathcal{T}} \mathbb{1}_{s_f \in \tau} F(\tau)}{\sum_{\tau \in \mathcal{T}} F(\tau)} = \sum_{\tau \in \mathcal{T}} \mathbb{1}_{s_f \in \tau} \pi_F(\tau) \quad (v)$$

by noting that $F(s_f) = \sum_{\tau \in \mathcal{T}} \mathbb{1}_{s_f \in \tau} F(\tau)$.

Table F: Complete Results on **Office-Home** with 5% labeling budget. **Boldface** and <u>underline</u> represent the best and second best scores.

Method	Ar —	→ Cl	$Ar \rightarrow Pr$		Ar -	→ Rw	Cl-	→ Ar	Cl-	→ Pr	$Cl \rightarrow Rw$		$\text{Pr} \rightarrow \text{Ar}$	
Method	Acc	JSD	Acc	JSD	Acc	JSD	Acc	JSD	Acc	JSD	Acc	JSD	Acc	JSD
Random	38.80	7.24	63.92	6.06	63.67	6.91	42.38	12.14	61.69	5.47	65.48	5.40	50.23	12.42
Entropy [50]	37.39	8.79	65.79	7.20	57.75	22.09	38.52	14.70	56.22	10.92	55.37	12.49	36.19	14.89
TQS [10]	43.55	6.15	68.94	8.38	64.47	5.37	39.39	11.37	59.63	6.12	54.00	7.74	45.03	11.81
CLUE [34]	42.14	7.12	70.12	5.88	65.12	4.78	41.57	7.54	63.11	7.23	56.23	7.17	48.14	9.54
EADA [52]	40.36	5.65	69.06	7.44	62.19	6.17	30.67	10.68	65.14	9.47	54.53	7.64	42.15	11.52
SDM-AG [53]	40.01	8.43	69.25	7.99	62.26	8.54	38.21	9.74	53.13	10.98	51.51	9.78	42.84	10.83
LAMDA [16]	42.19	8.59	59.75	7.22	<u>70.51</u>	9.25	<u>44.80</u>	17.49	<u>67.17</u>	6.21	<u>52.47</u>	10.21	43.75	10.88
RLADA (Ours) GFlowDA (Ours)	47.56 51.89	7.12 5.01	72.69 74.77	6.73 4.87	65.81 72.99	7.33 5.46	40.37 44.23	10.67 7.12	66.52 72.29	8.64 6.18	60.46 67.11	6.48 5.03	47.92 50.78	9.87 8.78

Method	Pr-	→ Cl	$Pr \rightarrow Rw$		$Rw \rightarrow Ar$		$Rw {\rightarrow} \ Cl$		$Rw \rightarrow Pr$		Avg	
Method	Acc	JSD	Acc	JSD	Acc	JSD	Acc	JSD	Acc	JSD	Acc	JSD
Random	45.80	7.08	51.25	7.18	40.39	11.01	41.91	6.23	60.89	5.94	52.20	7.76
Entropy [51]	40.56	15.91	57.29	18.16	37.46	17.79	41.09	15.44	56.73	18.22	48.36	14.72
TQS [9]	45.56	9.31	58.16	6.78	42.73	11.42	43.41	5.75	64.97	6.23	52.49	8.04
CLUE [34]	46.74	8.17	62.12	5.73	42.78	12.48	42.81	5.19	66.91	5.11	53.98	<u>7.16</u>
EADA [52]	40.22	7.53	55.94	14.28	42.15	16.88	36.13	5.60	64.85	8.95	50.28	9.32
SDM-AG [52]	40.92	8.81	55.81	12.12	40.65	10.42	39.25	7.33	60.69	11.92	42.84	10.83
LAMDA [16]	46.78	8.75	63.46	16.31	49.12	17.18	38.47	5.04	67.79	10.73	53.86	11.37
RLADA (Ours)	45.23	6.52	60.39	7.28	47.73	9.22	43.89	6.17	65.28	6.09	<u>55.32</u>	7.68
GFlowDA (Ours)	48.36	5.29	63.14	4.69	50.03	7.52	48.79	4.33	67.46	3.28	59.32	5.65

In addition, we define the backward transition probability

$$\mathcal{P}_B(s_t|s_{t+1}) = \frac{F(s_t \to s_{t+1})}{F(s_{t+1})},$$
 (w)

then we have

$$F(s_0) \prod_{t=0}^{f-1} \pi_F(s_{t+1}|s_t) = F(s_f) \prod_{t=0}^{f-1} \mathcal{P}_B(s_t|s_{t+1}), \quad (\mathbf{x})$$

where $F(s_f) = r(s_f)$.

By taking advantage of flow properties [3], we can describe the policy π based on the state space $\mathcal S$ and action space $\mathcal A$, and map them to the flow-based transition probabilities. In particular, let $\pi: \mathcal A \times \mathcal S \mapsto \mathbb R$ be the probability distribution $\pi(a|s)$ over actions $a \in \mathcal A$ for each state s, we can rewrite Eq.3 in the main text as follows

$$\pi(P_l) = \prod_{t=0}^{f-1} \pi(a_t | s_t) = \pi_F(s_f) \propto r(s_f) = r(P_s, P_t, P_l).$$

Hence, by exploiting the properties of the flow model, the policy can be constructed to be precisely proportional to the reward.

D. Algorithm

We provide the training procedure of GFlowDA in Algorithm 1.

E. Experiments

A. Dataset Setup under GUDA

We perform extensive experiments on four domain adaptation benchmarks including Office-31 [37], Office-Home [49], VisDA [33] and DomainNet [32], as well as a domain generalization benchmark, i.e., PACS [22]. To evaluate our algorithms on the GUDA setting, we modify the source and target domains by combining two subsampling protocols [54, 47] in order that the label spaces and label distributions across domains are both different. First, we remove samples belonging to some labels from the source and target domains separately in order to make the source and target label space different, i.e., to construct the common label space $\mathcal Y$ and private label space $\overline{\mathcal{Y}}_s$, $\overline{\mathcal{Y}}_t$. Then we consider only a small proportion of samples coming from the private label space and common label space to further modify the source and target domain. This yields label distribution especially for the common label space, i.e., $P_s(y) \neq P_t(y)$. Next, we describe the specific operations for each dataset separately.

Office-31: For Office-31, we use the middle 10 classes as the common label set, i.e., $\mathcal{Y}=\{10-19\}$, then in alphabetical order, the first 10 classes are used as the source private classes, i.e., $\overline{\mathcal{Y}}_s=\{0-9\}$, and the rest 11 classes are used as the target private classes, i.e., $\overline{\mathcal{Y}}_t=\{20-31\}$. Then we only consider 30% of source samples in common classes $\{0\text{-}4\}$ and private classes $\{10\text{-}14\}$.

Office-Home: For Office-Home, we use the middle 10 classes as the common classes, i.e., $\mathcal{Y} = \{30 - 39\}$. Then

Table G: Complete Results on PACS and VisDA with 1% target data as the labeling budget.

Malada	Α —	· C	$\mathbf{A} \to \mathbf{P}$		$A\toS$		С —	→ A	C -	→ P	$C\toS$		$P \to A$	
Method	Acc	JSD	Acc	JSD	Acc	JSD	Acc	JSD	Acc	JSD	Acc	JSD	Acc	JSD
Random	52.80	0.29	81.86	9.69	60.24	1.58	58.35	0.02	82.80	11.98	50.14	0.44	54.46	7.46
Entropy [50]	44.53	3.05	67.01	15.58	60.65	1.42	35.71	5.99	84.44	16.94	49.98	6.21	53.89	2.33
TQS [10]	63.82	5.82	83.89	5.71	80.43	2.77	44.48	4.39	87.65	3.47	74.76	2.27	58.77	11.08
EADA [52]	35.18	9.01	28.46	34.67	38.21	5.42	23.97	7.67	40.66	26.67	33.10	5.80	27.09	7.17
SDM-AG [53]	68.76	3.91	90.63	7.81	84.03	2.39	51.63	2.55	74.90	6.73	69.88	2.10	41.08	7.08
LAMDA [16]	53.20	1.62	82.67	6.66	55.87	2.96	58.81	1.04	91.08	9.81	46.37	2.31	60.21	3.05
RLADA (Ours) GFlowDA (Ours)	59.78 <u>64.34</u>	3.28 <u>1.06</u>	90.12 91.38	4.32 4.11	67.03 67.23	0.80 0.55	57.03 56.66	2.78 <u>0.61</u>	87.21 90.54	4.07 1.87	44.52 45.61	2.26 3.51	59.21 62.36	2.18 0.74

Mathad	P —	→ C	P -	→ S	S -	→ A	S -	→ C	S-	→ P	A	vg
Method	Acc	JSD	Acc	JSD	Acc	JSD	Acc	JSD	Acc	JSD	Acc	JSD
Random	60.36	6.62	71.87	3.05	49.65	2.52	53.81	4.84	82.88	3.10	63.27	4.30
Entropy [50]	63.82	6.78	79.98	2.24	45.76	3.40	50.07	16.55	64.74	17.86	58.38	8.20
TQS [10]	63.68	9.23	75.34	2.38	31.19	10.57	36.45	9.67	56.92	9.05	63.12	6.37
EADA [52]	24.77	7.69	20.98	5.04	46.04	5.51	40.25	5.31	53.87	14.01	34.38	11.16
SDM-AG [53]	58.46	4.49	74.84	4.31	43.00	1.74	46.53	1.05	54.18	6.04	63.16	4.18
LAMDA [16]	59.01	3.48	<u>76.73</u>	6.29	<u>62.41</u>	9.25	55.87	5.93	89.40	17.77	65.97	5.85
RLADA (Ours) GFlowDA (Ours)	58.41 64.03	3.81 2.92	58.57 59.03	2.16 1.99	62.20 63.15	2.85 3.12	59.32 61.82	1.41 1.03	88.57 93.02	5.32 1.66	66.00 68.26	2.94 1.93

the first 30 classes are used as the source private classes, i.e., $\overline{\mathcal{Y}}_s = \{0-29\}$. Correspondingly, the last 25 classes are used as the target private classes, i.e., $\overline{\mathcal{Y}}_t = \{40-64\}$. To construct a large label distribution, we consider 30% of source samples in common classes $\{0\text{-}14\}$ and private classes $\{30\text{-}34\}$, 30% of target samples in common classes $\{35\text{-}39\}$ and private classes $\{40\text{-}49\}$.

PACS: For PACS, we only consider one class labeled as "2" as the common label space to construct a large label space gap, which means that $\mathcal{Y}=\{2\}$. We use the first two classes as the source private classes denoted by $\overline{\mathcal{Y}}_s=\{0,1\}$ and use the last four classes as the target private classes denoted by $\overline{\mathcal{Y}}_t=\{3,4,5,6\}$. We consider 30% of source samples in class 0 and 30% of target samples in common class 2 and private class 3.

VisDA: For VisDA, we use classes 5 and 6 as the common classes denoted by $\overline{\mathcal{Y}}_s = \{5,6\}$. The first five classes are used as the source private classes denoted by $\overline{\mathcal{Y}}_s = \{0-4\}$. The last five classes are used as the target private classes denoted by $\overline{\mathcal{Y}}_t = \{7-11\}$. We consider 30% of source samples in common class 5 and source private classes $\{0,1,2\}$ and consider 30% of target samples in common class 5 and target private classes $\{7,8,9\}$.

DomainNet: For DomainNet, we use the first 150 classes as the common classes denoted by $\overline{\mathcal{Y}}_s = \{0-149\}$. The next 50 classes are used as the source private classes denoted by $\overline{\mathcal{Y}}_s = \{150-199\}$. The last 145 classes are used as the target private classes denoted by $\overline{\mathcal{Y}}_t = \{200-344\}$. We consider 30% of source samples in common classes $\{0.74\}$ and all source private classes and consider 30% of target samples in common classes $\{75.149\}$ and all target private

classes. We choose 3 domains to transfer between each other due to the large amount of data following [9].

B. Comparison Baselines

We compare GFlowDA with several popular active learning methods and active domain adaptation methods. Besides, since there are no reinforcement learning based algorithms in ADA literature, we also propose RLADA for comparison. Next, we describe the core idea of each method.

Random: The naive baseline that randomly selects several instances to annotate labels at each round.

Entropy [50]: Select instances for which the model has the highest predictive entropy.

TQS [10]: TQS is an ADA algorithm that selects the most informative samples by an ensemble of transferable committee, transferable uncertainty, and transferable domainness.

CLUE [34]: CLUE is an entropy-weighted clustering algorithm to take both the diversity and uncertainty of target data into a unified clustering framework.

EADA [52]: EADA is an energy-based sampling algorithm that incorporates both domain characteristics and instance uncertainty into every selection round.

SDM-AG [53]: SDM-AG is an effective ADA method consisting of a maximum margin loss and a margin sampling algorithm for data selection.

AUDA [16]: AUDA is the first ADA work under UniDA, which performs active learning towards target informative instances for unknown category inference.

LAMDA [16]: LAMDA is the first ADA work under label distribution shift. It is a distance based sampling strategy for choosing target data best preserves the entire target data

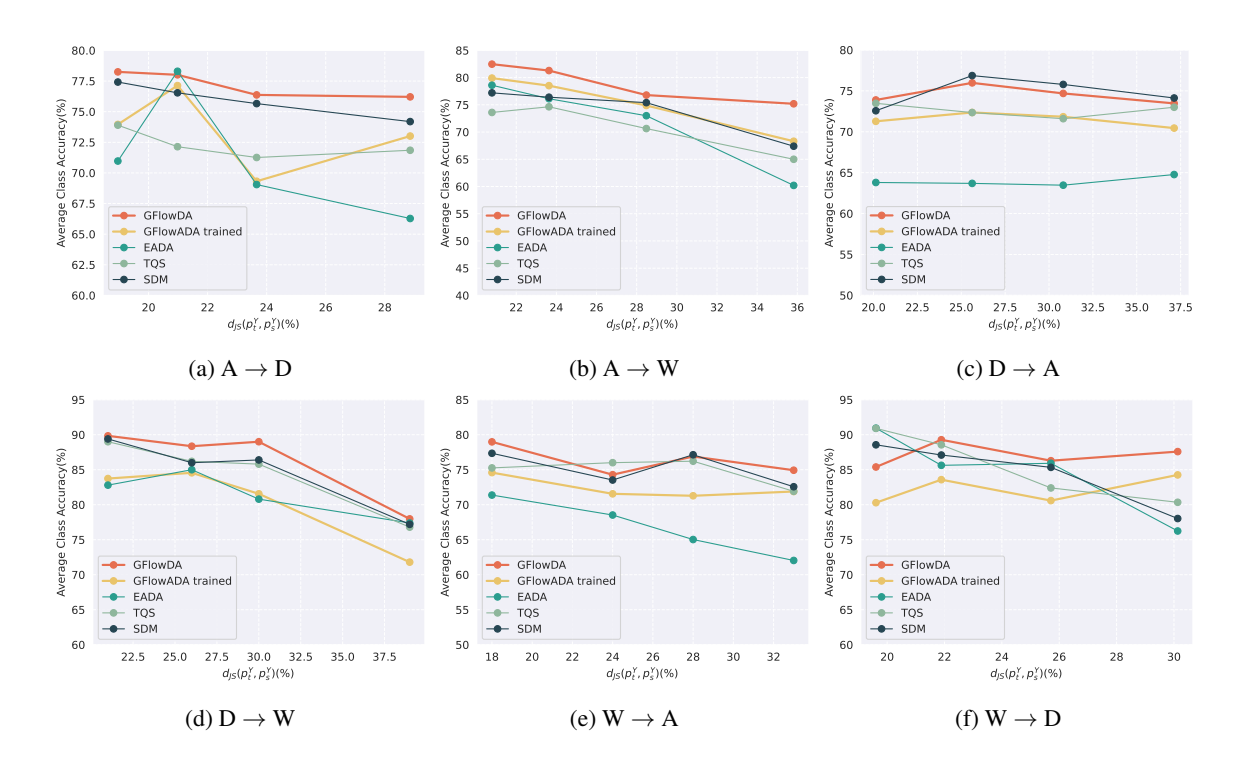


Figure I: Performance on Office-31 under different JSD values between the source distribution and the target label distribution.

Table H: Comparison resultson DomainNet dataset.

	P2	2R	S2	2R	R:	2S	Avg		
Method	Acc	JSD	Acc	JSD	Acc	JSD	Acc	JSD	
SDM-AG	30.12	23.23	28.18	20.64	20.18	26.19	26.14	23.35	
AUDA	35.13	19.45	36.56	19.29	22.81	21.44	31.50	20.05	
LAMDA	33.24	21.54	35.53	18.71	23.57	24.21	30.78	21.49	
GFlowDA	37.94	20.87	39.12	16.73	25.03	21.79	34.03	19.79	

distribution based on the MMD distance and uncertainty.

RLADA: RLADA is proposed by us to fill the gap of learning-based approaches in the ADA literature. We compare GFlowADA with RLADA to reflect the advantages of GFlowNet over traditional reinforcement learning algorithms such as Proximal Policy Optimization(PPO) [42].

C. Implementation details

In this subsection, we introduce the implementation details of the domain adaptation model and policy network model.

Domain Adaptation Model: For Random, Entropy, LAMDA and GFlowDA, we apply ResNet50 [13] models pre-trained on ImageNet [20] as a feature extractor. We use Adadelta optimizer training with a learning rate of 0.1 and a batch size of 32. The classifier is implemented by a

fully-connected layer. The domain discriminator contains a fully-connected layer and a sigmoid activation layer. For other active domain adaptation methods, we use default hyperparameters and network architecture introduced in their works except that keeping using ResNet50 pretrained on ImageNet as the backbone. We train 1 epoch in the training process for GFlowDA and 40 epochs for other baselines.

Policy Network Model: For GFlowDA and RLADA, we implement the policy network as a two-layer MLP with a hidden layer size of 8. We use Adam as the optimizer with a learning rate of 0.001. The policy network is trained for a maximum of 2000 episodes with a trajectory size of 5. All methods are implemented based on PyTorch, employing ResNet50 [13] models pre-trained on ImageNet [20]. Besides, we run each experiment three times and report mean accuracies and JSD values.

D. More Results

Performance of GFlowDA. Table **F** and Table **G** present the complete experimental results of GFlowDA and compared baselines on all subtasks of the Office-Home and PACS datasets. Table **H** shows the results of GFlowDA and three main SOTA methods on three subtasks of the DomainNet dataset. These tables demonstrate the superiority and robustness of GFlowDA, which outperforms other methods in all datasets including two large-scale datasets.

Transferability of GFlowDA. Fig. I represents the trans-

ferability of our method compared with existing ADA methods in six subtasks on Office-31. Specifically, we train our GFlowDA with $d_{\rm JS}(P_s^Y,P_t^Y)=0.38$. Then the learned active policy network is applied to four target sample sets belonging to the same domain with different JSD distances $d_{\rm JS}(P_s^Y,P_t^Y)$ from the source label distribution, as shown on the x-axis of Fig. I. These sample sets are constructed by randomly subsampling on the original target dataset. Experimental results demonstrate that our GFlowDA can directly transfer to new tasks even without pre-training, and its performance surpasses non-learning based methods in most cases. Rather than maximizing cumulative reward, we focus more on the consistency of action probabilities with the true reward distribution.